



1 **Rising atmospheric CO₂ concentrations: the overlooked factor promoting SW Iberian**
2 **Forest development across the LGM and the last deglaciation?**

3

4 Gomes, Sandra.D.^{a,b,c*}

5 Fletcher, William.J.^a

6 Stone, Abi^a

7 Rodrigues, Teresa^{b,c}

8 Rebotim, Andreia^{b,c}

9 Oliveira, Dulce^{b,c}

10 Sánchez Goñi, Maria. F.^{d,e}

11 Abrantes, Fatima^{b,c}

12 Naughton, Filipa^{b,c}

13

14 ^aQuaternary Environments and Geoarchaeology, Department of Geography, School of
15 Environment, Education and Development, The University of Manchester, Manchester,
16 Oxford Road, Manchester, M13 9PL, United Kingdom;

17 ^bDivisão de Geologia e Georecursos Marinhos, Instituto Português do Mar e da Atmosfera
18 (IPMA), Rua Alfredo Magalhães Ramalho 6, 1495-006 Lisboa, Portugal;

19 ^cCentro de Ciências do Mar (CCMAR), Universidade do Algarve, Campus de Gambelas, 8005
20 - 139 Faro, Portugal;

21 ^dÉcole Pratique des Hautes Études, EPHE, PSL Université, Paris, France;

22 ^eEnvironnements et Paléoenvironnements Océaniques et Continentaux, UMR 5805,
23 Université de Bordeaux, Pessac, France.

24

25

26 *Corresponding author: E-mail: sandra.domingues@manchester.ac.uk (Sandra Domingues
27 Gomes); Address: Quaternary Environments and Geoarchaeology, Department of
28 Geography, School of Environment, Education and Development, The University of
29 Manchester, Manchester, Oxford Road, Manchester, M13 9PL, United Kingdom

30

31

32

33

34

35

36

37

38

39



40 **Abstract:**

41 Across the last deglaciation, the global atmospheric concentration of carbon dioxide ($p\text{CO}_2$)
42 increased from ~180 to ~280 ppm. However, the impact of $p\text{CO}_2$ changes on vegetation
43 across the last deglaciation remains poorly understood. Under full glacial low $p\text{CO}_2$, plants
44 experienced constraints on photosynthesis. Therefore, a significant reduction in $p\text{CO}_2$
45 limitation should have impacted local and regional vegetation dynamics across deglaciation.
46 We hypothesise that deglacial $p\text{CO}_2$ rise could have (1) led to a gradual reduction of the
47 physiological constraint promoting forest response when moisture availability was sufficient,
48 despite low temperatures; and (2) amplified the response of forest development to warmer
49 and wetter conditions. The high-resolution analysis of terrestrial (pollen, $\text{C}_{29}:\text{C}_{31}$ organic
50 biomarker) and marine (alkenone-derived Sea Surface Temperature, $\text{C}_{37}:4\%$, and long-chain
51 n-alkanes ratios) indicators, using a direct land-sea direct comparison, in the Iberian margin
52 site Integrated Ocean Drilling Program (IODP) U1385 ("Shackleton site") throughout the Last
53 Glacial Maximum (LGM) and last deglaciation allowed us to track and compare the changes
54 with shifts in global $p\text{CO}_2$. The LGM is characterised by a grassland-heathland mosaic type
55 ecosystem, triggered by cool and moderately humid conditions but low $p\text{CO}_2$ levels may have
56 exacerbated physiological drought and suppressed forest development. During Heinrich
57 Stadial 1 (HS1) the coldest and most arid conditions combined with sustained low $p\text{CO}_2$ values
58 precluded forest development and resulted in the dominance of Mediterranean steppe or semi-
59 desert vegetation. The Bølling-Allerød (BA) is characterised by a temperature optimum
60 (warmest SSTs and forest development) and variable moisture condition, while increasing
61 $p\text{CO}_2$ which contributed to the highest levels of forest development. Within the BA, significant
62 SW Iberian forest development occurred at ~15 cal kyr B.P. associated with an increase in
63 $p\text{CO}_2$ above 225 ppm. During the Younger Dryas (YD), cool temperatures combined with
64 sufficient moisture availability allowed the maintenance of a grassland-forest mosaic, the
65 increasing values of $p\text{CO}_2$ in this period should have offset the low temperature as well as the
66 moisture levels and allow the forest to persist. The overlooked role of $p\text{CO}_2$ could explain an
67 intriguing feature observed in Site U1385 and other Iberian margin records, namely the near
68 absence of forest during the LGM and HS1 but relatively high forest cover during the YD. Our
69 study aims to shed light on the influence of climatic factors (temperature and moisture
70 availability) together with $p\text{CO}_2$ as thresholds on forest response to deglacial climate changes
71 across the Iberian Peninsula.

72

73 **Keywords:**

74 Iberian margin; Deglaciation; LGM; Direct sea-land comparison; climatic space; Climatic
75 parameters vs $p\text{CO}_2$; Forest development; Pollen analysis

76 **1. Introduction**

77 The last deglaciation is characterised by a series of "classic" abrupt climate events, being one
78 of the periods widely studied for its particular succession of cold and warm events (Alley and
79 Clark, 1999; Lynch-Stieglitz, 2007; Fletcher et al., 2010a; 2010b; Salgueiro et al., 2014;
80 Marcott et al., 2014; Martrat et al., 2014; Naughton et al., 2016; Ausín et al., 2020). While
81 some records based on direct sea-land comparison are available for SW Iberian margin
82 (Boessenkool et al., 2001; Turon et al., 2003; Chabaud et al., 2014; Oliveira et al., 2018;
83 Naughton et al., 2019), few exist that cover the entire deglaciation, and none have the required
84 resolution or chronological precision to detect abrupt vegetation and climate shifts in detail.
85 The high temporal resolution, direct sea-land comparison provided by Site U1385 enables,



86 therefore, the detection of significant vegetation and climatic shifts in SW Iberia across the last
87 deglaciation.

88 The interactions between the lithosphere, hydrosphere (oceanic and terrestrial), cryosphere
89 and atmosphere during extreme climate events are crucial to understanding the climate
90 system behaviour. The last deglaciation, from 21 to 6 ka, was accompanied by a global
91 temperature increase of 5 to 10°C, depending upon the latitude (Bard et al., 1987; Alley and
92 Clark, 1999; Clark et al., 2012), although the warming was not continuous. Two major abrupt
93 climatic cooling episodes, associated with ocean-atmospheric perturbations were
94 superimposed on the warming trend, the Heinrich Stadial 1 (HS1) and the Younger Dryas
95 (YD), bracketing the intervening Bølling-Allerød (BA) interstadial. During the last deglaciation,
96 global atmospheric concentrations of carbon dioxide (pCO₂) increased from ~180 ppmv to 280
97 ppmv (Monnin et al., 2001; Shakun et al., 2012; Marcott et al., 2014), being among the highest
98 amplitude shifts in pCO₂ of the last 800,000 years (Lüthi et al., 2008). The high-temporal
99 resolution West Antarctic Ice Sheet Divide ice core furthermore shows three main rapid (< 200
100 years) pCO₂ rises, each of ~10 to 15 ppmv, which took place at the end of HS1; within the BA
101 and at the onset of the YD (Marcott et al., 2014).

102 The role of CO₂ as a climate driver throughout the ice ages is still intensely debated; however,
103 it has been mainly considered as either (1) a primary driver of the climatic changes, in which
104 the CO₂ led the temperature records in Northern Hemisphere (Shakun et al., 2012; Marcott
105 et al., 2014); (2) an amplifier responding as positive feedback to the warming (Alley and Clark,
106 1999; Clark et al., 2012); or (3) as a consequence rather than a cause of climatic changes
107 (Denton et al., 2010). Besides its impact on climate, the physiological influence of pCO₂ as a
108 limiting factor over plant development on Quaternary timescales has also been discussed
109 (Cowling and Sykes 1999; Crucifix et al., 2005; Ward et al., 2005; Gerhart and Ward, 2010;
110 Harrison and Sanchez Goñi, 2010). However, its role is often neglected, for example in
111 vegetation-based climate reconstructions which do not account for pCO₂ effects (e.g. Elenga
112 et al., 2000; Sánchez Goñi et al., 2002; Peyron et al., 1998; Fletcher et al., 2010a; Bartlein et
113 al., 2011; Tarroso et al., 2016).

114 The annual exchange of CO₂ between the atmosphere and biosphere due to photosynthetic
115 activity corresponds to more than one-third of the total pCO₂ stored in the atmosphere
116 (Farquhar and Lloyd, 1993). The study of increased plant growth and global vegetation
117 greening under higher concentrations of pCO₂ (CO₂ fertilisation) is very topical within
118 discussions of current global climate change (e.g. Piao et al., 2019) whilst the inverse scenario
119 (low pCO₂) has received less attention. The influence of lowering pCO₂ on vegetation has
120 been examined in coupled climate-vegetation models (e.g. Harrison and Prentice, 2003; Sitch
121 et al., 2003; Crucifix et al., 2005; Ramstein et al., 2007; Wu et al., 2007; Prentice and Harrison
122 2009; Bartlein et al., 2011; Woillez et al., 2011; Svenning et al., 2008; 2011; Claussen et al.,
123 2013; Prentice et al., 2017; Shao et al., 2018; Cao et al., 2019). It has been suggested that
124 pCO₂ changes play an essential role on the development of vegetation (Wu et al., 2007), its
125 coverage (e.g. Harrison and Prentice 2003; Woillez et al., 2011; Harrison et al., 2016; Cao et
126 al., 2019), vegetation productivity (Claussen et al., 2013) and water use efficiency (WUE)
127 (Polley et al., 1995; Cramer et al., 2001).

128 The role of pCO₂ in plant physiology is well known, in particular during photosynthesis, but the
129 magnitude of its influence on the composition and distribution of past vegetation remains
130 poorly understood. Under low pCO₂ concentrations, stomatal conductance and stomatal
131 density must increase to maintain an adequate CO₂ gradient between the atmosphere and the
132 leaf during photosynthesis. The evaporative demand increases and higher amounts of water
133 are lost through transpiration, reducing WUE and imposing a physiological drought (Street-



134 Perrot et al., 1997; Körner, 2000). One should expect that the CO₂ limitations on plant
135 development are, and were, not globally or temporally uniform, depending mainly on the
136 regional level of water-stress. The particular influence of CO₂ limitations in arid and semi-arid
137 areas is highlighted by evidence for global greening of arid areas due to CO₂ fertilisation
138 (Randall et al., 2013). Global evidence supports an atmospheric CO₂ fertilisation effect,
139 especially trees growing in drought-stressed conditions which benefit from increased WUE to
140 enhance growth (Huang et al., 2007). Nevertheless, at local scales, nutrient limitations may
141 limit the response of vegetation to rising CO₂ (e.g. Tognetti et al., 2008). The Mediterranean
142 region, with its characteristic annual hydrological deficit and seasonal water stress, is a key
143 place for exploring the potential role of pCO₂ limitation on vegetation growth. Therefore, past
144 vegetation dynamics in this region may be considered as a significant (inverse) analogue to
145 understand the current impact of increasing temperature and pCO₂ within semi-arid and arid
146 ecosystems.

147 Vegetation changes across the Iberian Peninsula for the last deglaciation as recorded in
148 palaeoecological proxies are traditionally interpreted as a result of the combined effects of
149 temperature, precipitation and evaporation changes (e.g. Peyron et al., 1998; Carrión et al.
150 2002; Sánchez Goñi et al., 2002; Combourieu Nebout et al., 2009; Dormoy et al., 2009;
151 Fletcher et al., 2010a; Arranbari et al., 2014; Bartlein et al., 2011; Naughton et al., 2011; 2019;
152 Tarroso et al., 2016). The majority of climate reconstructions and simulations for glacial
153 periods based on vegetation records do not consider the influence of CO₂ and may, therefore,
154 be biased when the effect of pCO₂ is not included. Palaeovegetation (pollen-based) data is
155 vital for testing climate model simulations, both as temporal trends and reconstructions of
156 spatial distributions (Prentice et al., 1992; 2001; Jolly and Haxeltine, 1997; Harrison and
157 Prentice, 2003; Bartlein et al., 2011; Prentice et al., 2011; Harrison et al., 2016; Cao et al.,
158 2019). Within this, reconstructions of vegetation assemblage (Elenga et al., 2000; Svenning
159 et al., 2008) and quantitative estimates of climatic variables (Wu et al., 2007; Svenning et al.,
160 2008; Prentice et al., 2017) are both critical. It is essential to recognise that pCO₂ is correlated
161 with WUE or the balance between carbon assimilation and transpiration (water loss).
162 Neglecting this influence may contribute to the unreliability of precipitation reconstructions,
163 specifically underestimation of past precipitation under full glacial conditions (Jolly and
164 Haxeltine, 1997; Cowling and Skyes, 1999; Gerhart and Ward, 2010; Prentice et al., 2017;
165 Cleator et al., 2020). In contrast, the influence of CO₂ on forest development in the southwest
166 Iberian Peninsula under interglacial conditions may be negligible compared with precipitation
167 changes, as recently revealed by transient model experiments (Oliveira et al., 2018).

168 The need for additional regional-based palaeoecological studies, such as for the southwest
169 Iberian Peninsula, is highlighted in a recent model-data comparison using the BIOME4 model
170 and a biome-scale reconstruction compiled from pollen records across the Northern
171 Hemisphere (> 30°N), which reveals a level of unexplained variability in patterns across both
172 space and time (Cao et al., 2019). Detailed pollen assemblage datasets may provide key
173 insights into other factors than temperature, precipitation and potential evaporation that drive
174 changes in vegetation dynamics and composition, such as pCO₂ (Ludwig et al., 2018; Cao et
175 al., 2019). The importance of pCO₂ during periods of abrupt change, such as the ones that
176 occurred in the SW IP during the deglaciation, deserves particular attention. Understanding
177 the temporal dynamics of the regional forest cover, hereafter TMF (Temperate and
178 Mediterranean Forest), requires exploration of the role of different parameters (temperature,
179 precipitation and CO₂). The new multiproxy study of Site U1385 allows the direct comparison
180 between terrestrial and marine climatic indicators across the LGM and deglaciation at high
181 (centennial-scale) temporal resolution, and therefore, the detailed reconstruction of abrupt



182 changes in the vegetation-based atmospheric conditions and SSTs over the SW Iberian
183 margin, as well as its comparison with available Iberian records. The aims of this study are to:
184 a) Document terrestrial and marine responses to past climate changes at centennial-
185 scale resolution for the LGM and last deglaciation, including the main abrupt events of
186 the last deglaciation (HS1; B-A and YD) at Site U1385A;
187 b) Explore the main factors driving forest development during the LGM and last
188 deglaciation;
189 c) Evaluate the evidence for indications of pCO₂ thresholds for forest development.

191 2. Materials and environmental setting

192 [Figure 1]

193
194 IODP Site U1385 is a composite record of four drillings in the SW Iberian margin (37°34.285'N;
195 10°7.562'W, 2587 m below sea level - mbsl) located on a spur at the continental slope of the
196 Promontorio dos Principes de Avis, which is elevated above the abyssal plain and free from
197 turbidite influence (Hodell et al., 2015) (Fig. 1). This work focuses on Hole A, a continuous
198 record of 10 corrected revised meter composite depth (crmcd) mainly composed of
199 hemipelagic silt alternating with clay (Hodell et al., 2015). For this study, Hole A was sampled
200 from 3.84 to 1.08 crmcd, which corresponds to the period between 22550 and 6480 cal yr BP.
201 The sediment supply, including pollen grains, to Site 1385 is mainly derived via fluvial
202 transport from the the Tagus and Sado hydrographic basins, providing a reliable signature of
203 the vegetation of the adjacent continent (Naughton et al., 2007; Morales-Molino et al., 2020).
204 The present-day climate of southwestern Iberia is characterised by a Mediterranean climate
205 strongly influenced by the Atlantic Ocean, Köppen classification CSa with warm summers
206 (around 22°C as the average temperature of the warmest month) mean annual temperatures
207 between 12.5°C and 17.5°C, and mean annual precipitation from 400 to 1000 mm/yr. The
208 rainy season peaks in the winter between November and January and drought occurs in the
209 summer generally from June to September.

210 3. Methods

211 3.1. Chronological framework

212 [Table 1, Figure 2, Figure 3, S.M. Fig. 1]

213
214
215 Eleven AMS ¹⁴C dates were used to generate a new age-model for the last deglaciation at
216 Site U1385 (Table 1 and Fig. 2). Five previously published AMS ¹⁴C dates from Oliveira et al.
217 (2018) (analysed at the Vienna Environmental Research Accelerator (VERA), Isotope Physics
218 Research Group, University of Vienna, Austria, from monospecific foraminifer samples of
219 *Globigerina bulloides*) were also used (Table 1). A new set of six samples for AMS ¹⁴C were
220 selected and processed at the Keck Carbon Cycle AMS Facility, (University of California,
221 Irvine), from monospecific foraminifer samples of *Globigerina bulloides* (Table 1). The new
222 age-model was calculated using a Bayesian approach, through the software Bacon
223 implemented in R (Blaauw and Christen, 2011; R Development Core Team, 2020). We used
224 the Marine13.14d calibration curve (Reimer et al., 2013) which integrates a marine reservoir
225 correction (R) of 500 ± 200 years (Bard et al., 2004a; 2004b; 2013). We calculate a weighted
226 mean DeltaR, based on the ten neighbouring sites (around Site U1385) of 143 ± 139 years,
227 at 1 s.d using CALIB 7.1 (Stuiver et al., 2020) to account for regional effects.

228 3.2. Pollen analysis



230

231 A total of 97 samples (including 25 previously published by Oliveira et al., 2018) were analysed
232 between 3.84 to 1.08 crmcd in Hole A, and prepared at the University of Bordeaux using the
233 standard protocol of the the UMR EPOC laboratory The sediment was firstly separated using
234 coarse-sieving at 150 µm, retaining the fine fraction. A sequence of chemical treatments,
235 starting with cold HCl at increasing concentrations (10%, 25%, 50%) eliminated calcium
236 carbonate particles. Cold HF. at increasing strength (45% and 70%) eliminated silicates. The
237 remaining residue was micro-sieved (10 µm mesh), retaining the coarse fraction. Exotic
238 *Lycopodium* spore tablets of known concentration were added to each sample to calculate
239 pollen concentrations (Stockmarr, 1971). The obtained residue was mounted in a mobile
240 medium composed of phenol and glycerol 1% (w/v), to allow the pollen/spore rotation and
241 accurate identification. Samples were counted using a transmitted light microscope at 400X
242 and 1000X (oil immersion) magnifications. To perform pollen identification, we used
243 identification keys (Faegri and Iversen, 1989; Moore et al., 1991), a photographic atlas (Reille,
244 1992; 1995) and the SW Mediterranean modern reference collection.

245 The total count ranged from 198 to 1545 pollen and spores per sample, with a minimum of
246 100 terrestrial pollen grains and 20 pollen morphotypes to provide statistical reliability of the
247 pollen spectra (McAndrews and King, 1976; Heusser and Balsam, 1977). The main pollen
248 sum was calculated following previous palynological studies of Site U1385 (e.g. Oliveira et al.,
249 2016) that excluded *Pinus*, *Cedrus*, aquatic plants, Pteridophyte and other spores, and
250 indeterminable pollen. The pollen percentages are calculated against the main pollen sum;
251 *Pinus* and *Cedrus* percentages as well local taxa are calculated against the main pollen sum
252 plus the taxon. *Pinus* pollen, being an anemophilous taxon, is generally overrepresented in
253 marine deposits and therefore excluded from the main sum (Naughton et al., 2007). *Cedrus*
254 being an exotic component possibly transported by wind from the Atlas Mountain (Morocco),
255 is also excluded. PSIMPOLL 4.27 (Bennett, 2009) was used to plot percentages for selected
256 taxa, grouped by ecological affinities (Gomes et al., 2020). Stratigraphically constrained
257 cluster analysis by Sum of Squares (CONISS) determined the five statistically significant
258 pollen assemblage zones (CONISS) (U1385-1 to 5) based on a dissimilarity matrix of
259 Euclidean distances with pollen taxa $\geq 1\%$ (Grimm, 1987; Bennet et al., 2009).

260

261 3.3. Compilation of Iberian margin pollen records

262

263 In order to assess vegetation and climate changes in the IP region across the LGM and the
264 last deglaciation, we compiled available marine records along the Iberian margin covering the
265 period from 23 to 6 ka. Pollen count datasets from eight pollen records (D13882 - Gomes et
266 al. 2020; MD03-2697 - Naughton et al., 2016; MD95-2039 – Roucoux et al., 2005; MD95-2043
267 Fletcher and Sánchez Goñi, 2008; MD95-2042 – Chabaud et al., 2014; ODP Site 976 –
268 Comborieut Nebout et al., 1998; 2002; 2009; SU81-18 Turon et al., 2003; Site U1385 – this
269 study) were used with the original published chronologies. Pollen percentages were
270 recalculated against the main pollen sum. A uniform calculation of the pollen-based ecological
271 group TMF was made for each record, integrating the following taxa of 1) Temperate trees and
272 shrubs: deciduous *Quercus*, *Acer*, *Betula*, *Cannabis/Humulus*, *Carpinus*, *Castanea*, *Fraxinus*
273 *excelsior-type*, *Hedera helix*, *Hippophae*, *Ilex*, *Juglans*, *Myrica* and *Vitis*; and 2) Mediterranean
274 taxa: evergreen *Quercus*, *Quercus suber*, *Arbutus type*, *Buxus*, *Daphne*, *Jasminum*,
275 *Ligustrum*, *Myrtus*, *Olea*, *Phillyrea*, *Pistacia*, *Rhamnus*, *Rhus*.

276 To assess the general trend of vegetation patterns throughout the deglaciation, we applied a
277 Generalised Additive Model (GAM), considered as a more robust statistical approach than



278 loess curves (Wood, 2017; Simpson, 2018). The GAM model was fitted using the *gam()*
279 function of the *mgcv* package (version 1.8.24; Wood, 2017) for R (version 3.6.3; R Core Team,
280 2020). We fitted the model using a standard GAM with REML smoothness selection, with 30
281 basis functions ($k=30$) and a smoothing parameter of 0.0001 ($sp=0.0001$). To check the
282 validity of the smooth terms and if the used basis functions captured the wiggleness, we applied
283 a test using the *gam.check()* function of the *mgcv* package. The *k-index* obtained higher than
284 1, and the *p-value* supported the hypothesis that in both cases, enough basis functions were
285 used. The curve shows the fitted GAMs for TMF with an approximate 95% confidence interval
286 (Simpson, 2018).

287

288

289 **3.4. Molecular biomarkers**

290

291 Marine biomarker analyses were carried out in 123 levels, including 30 already published by
292 Oliveira et al. (2018). All analyses were performed following the extraction and analytical
293 methods described in Villanueva et al. (1997) and Rodrigues et al. (2017).

294 Marine coccolithophorid algae synthesise organic compounds including alkenones (Volkman
295 et al., 1980) (Fig. 3i and j). Seawater temperature changes influence the amounts of di-, tri-
296 and tetra-unsaturated alkenones produced by algae (Brassell et al., 1986). The use of organic
297 solvents to separate the total lipid fraction from sediments allows the sea surface temperature
298 alkenone-based reconstruction ($U^{k_{37}} - SST$) (e.g. Rodrigues et al., 2017, Villanueva and
299 Grimalt, 1997). The $U^{k_{37}}$ index (Prahl and Wakeman, 1987) was converted to temperatures
300 values using the global calibration equation defined by Müller et al. (1998) with an uncertainty
301 of 0.5°C (Grimalt et al., 2001). Additionally, tetra-unsaturated alkenone ($C_{37:4}$) percentages
302 were calculated due to their potential to identify the occurrence of cold freshwater pulses
303 associated with iceberg discharges (Bard et al., 2000; Martrat et al., 2007; Rodrigues et al.,
304 2011, 2017) and therefore, changes in the reorganisation of surface water masses in the North
305 Atlantic (Rodrigues et al., 2017).

306 The ratio between C_{29} and C_{31} *n*-alkanes was also calculated to understand how epicuticular
307 wax production in terrestrial plants varied through the time (Eglinton and Hamilton 1967). This
308 index is generally considered to encompass the dynamic between woody plants vs grasses
309 plants of the adjacent continent (Cranwell 1973, Tareq et al., 2005, Bush et al., 2013). If the
310 index is >1 , it is typically considered to reflect higher quantities of C_{29} *n*-alkanes by trees and
311 shrubs, while value of the index <1 are generally considered to indicate the production of
312 higher quantities of C_{31} *n*-alkanes by grasses and herbaceous plants (Cranwell, 1973; Ortiz et
313 al., 2010; Rodrigues et al., 2009). This relation encompasses the adaptation of plants, by
314 increasing leaf wax production, to reduce water loss during the photosynthetic processes and
315 prevent desiccation promoted by harsh winds or more arid conditions (Bush and McInerney,
316 2013).

317

318

319 **4. Results and interpretation**

320

321 **4.1. Age model**

322

323 The studied interval encompasses the period from ~23 to 6 ka, as shown by the radiocarbon
324 age model (Fig. 2). The average temporal resolution for the pollen and marine biomarkers



325 across the deglaciation is 127 and 116 years, respectively, or slightly lower (171 and 131
326 years, respectively) when including the Holocene section (Fig. 3 and S.M. Fig. 1).

327

328 **4.2. Major vegetation and climatic shifts in SW Iberia during the last deglaciation**

329

330 The U1385 pollen diagram with clustering analysis (SM Fig.1) and SST profile reveals four
331 main episodes over the LGM and the last deglaciation (Fig. 3, further details in S.M. Table 1).
332 We emphasise the findings of the new U1385 record but also showcase the excellent
333 correspondence between the record and the Iberian margin compilation (Fig. 3c), highlighting
334 generally strong parallels in forest development across the compilation of eight records:

335 Pollen zone U1385-1 (22550 – 18130 cal yr B.P.) corresponds to the LGM, and shows the
336 dominance of semi-desertic taxa (STE, ~40%), reflecting dry conditions over the continent
337 (Fig. 3d). The high values of $C_{29/C_{31}}$ between 0.8 and 1 detected during this interval, might
338 suggest an increase in epicuticular wax production by woody plants in response to dry
339 conditions (Fig. 3h). Although STE were the dominant taxa, the moderate presence of
340 heathland (ERI, ~10-20%) suggests some moisture availability (Fig. 3e) as at present-day they
341 develop preferentially under oceanic (temperate and moist) climate (e.g. Polunin and Walters,
342 1985). The low percentages of TMF (5-15%) (Fig. 3c), suggesting cold and dry conditions
343 over the continent, are consistently observed across the marine records in southerly locations
344 off the Iberian Peninsula (MD95-2043 - Fletcher and Sánchez Goñi, 2008 and ODP Site 976
345 - Comborieut Nebout et al., 1998; 2002; 2009 in the Mediterranean Sea, and SU81-18- Turon
346 et al., 2003 in the Atlantic Ocean) as well as further North off the IP (MD99-2331 and MD03-
347 2697- Naughton et al., 2007; 2016). This zone is also characterised by moderately cool SSTs
348 (average ~14.5°C, Fig. 3j), and minor influence of meltwater pulses as revealed by the low
349 (not significant, < 2%) $C_{37:4}$ values (Fig. 3i).

350 Pollen zone U1385-2 (18130 – 15400 cal yr B.P.) corresponds to HS1, and reveals the
351 maximum expansion of STE (Fig. 3d) suggesting extreme dry conditions over the
352 southwestern Iberian Peninsula. The decrease observed in more moisture-demanding heaths
353 (ERI) as well as terrestrial marshes and wetlands (decrease in *Isoetes* undiff.) could be likely
354 the result of increased moisture stress (Fig. 3e, S.M. Table 1 and S.M. Fig. 1). The high $C_{29/C_{31}}$
355 values (mostly above 1) observed consistently in this zone suggest a further increase in
356 epicuticular wax production by the vegetation cover as compared with the preceding LGM
357 (Fig. 3h). At the same time, the TMF, and especially the thermophilous components, almost
358 disappeared, confirming dry but also extreme conditions (Fig. 3c and f, S.M. Fig. 1 and S.M.
359 Table 1). The dominance of STE during HS1 is consistent across the majority of the IP records
360 (Roucoux et al., 2005; Naughton et al., 2007; 2016; MD95-2043 - Fletcher and Sánchez Goñi,
361 2008; ODP Site 976 – Comborieut Nebout et al., 2002). In conjunction, SSTs drop to minimum
362 values (~12°C, Fig. 3j), reflecting the coldest sea surface conditions of the deglaciation in SW
363 Iberian margin. The high $C_{37:4}$ values (~8.2%, Fig. 3i) reflect maxima of meltwater pulses,
364 associated with extreme cold conditions and a clear expression of HS1 in the Atlantic Ocean.
365 Pollen zone U1385-3 (15400 – 12760 cal yr B.P.) shows a strong development of TMF
366 including a minor increase in Mediterranean elements (Fig. 3c and f) and a reduction of STE
367 (Fig. 3d) reflecting a trend of increasing warmth and humidity marking the Bølling-Allerød
368 episode in the southwestern Iberian Peninsula. Although STE decreases at the onset of this
369 episode, grasses expand, suggesting still relatively dry conditions during the beginning of this
370 episode (Fig. 3g and d). The increase of SSTs parallels the terrestrial/atmospheric warming
371 trend (Fig. 3j and c, although the maximum SST (17.5°C) was attained before maximum TMF
372 expansion. The asynchrony, observed at the onset of this zone, between TMF (gradual



373 increase, Fig. 3c) and SST (maximum values, Fig. 3j) could indicate some moisture deficit at
374 the start of this zone, and this assumption can be supported not only by the high abundance
375 of grasses but also by the continued high C_{29}/C_{31} ratio at the onset of this interval (Fig. 3g and
376 h). Indeed, several other pollen records across IP show a similar pattern of dryness during the
377 initial phase of the BA (Van der Knaap and van Leeuwen, 1997; Roucoux et al., 2005;
378 Naughton et al., 2007; 2016; ODP Site 976 – Comborieut Nebout et al., 2002). The most likely
379 explanation for the delayed response of the TMF is the existence of a moisture deficit at the
380 start of the BA (Naughton et al., 2016). The rise in Mediterranean elements towards the end
381 of the zone suggests an increasing expression of warm but dry summers. The high C_{29}/C_{31}
382 ratio at the onset of this zone shifts towards low values by the end of this episode, possibly
383 reflecting an overall decrease of wax production by plants in response to reduced aridity (Fig.
384 3h).

385 Pollen zone U1385-4 (12760 – 11050 cal yr B.P.) corresponds to the YD and initial Holocene.
386 This zone is marked by a TMF contraction and expansion of STE (Fig. 3c and d), reflecting
387 regional cooling and drying over the southwestern Iberian Peninsula. There is a slight increase
388 registered by the C_{29}/C_{31} ratio, consistent with the patterns observed in preceding zones which
389 could again be associated with an increase in the leaf wax production under more arid
390 conditions (Fig. 3h). A significant SST reduction is observed with a minimum of 13.2 °C in the
391 record (Fig. 3j). However, in contrast to HS1, freshwater pulses are insignificant during this
392 phase (Fig. 3i). The fairly weak reduction in TMF observed in our record and corroborated
393 by the compiled records (Fig 3c) contrasts with the steppe environment described for this
394 interval, especially in the southeast of the IP (Carrión et al., 2002; Camuera et al., 2019). A
395 more pronounced forest contraction is observed in the high altitude terrestrial/lacustrine cores
396 (Quintanar de la Sierra II – Peñalba et al., 1997; and La Roya - Allen et al., 1996) in which the
397 near-disappearance of the forest might reflect the altitudinal adjustments in vegetation belts
398 (Aranbarri et al., 2014). However, the U1385 record and other Iberian margin and IP records
399 (e.g. Lake de Banyoles – Perez-Obiol and Julià, 1994; MD03-2697 – Naughton et al., 2007;
400 MD95-2039 – Roucoux et al., 2005; Charco da Candieira – van der Knaap and van Leeuwen,
401 1997; MD95-2042 – Chabaud et al., 2014; D13882 - Naughton et al., 2019; MD95-2043-
402 Fletcher and Sánchez Goñi, 2008; ODP Site 976 – Comborieut Nebout et al., 2002) show a
403 relatively high percentage of TMF during the YD when compared with the previous HS1 in the
404 SW IP (Fig. 3c).

405 Pollen zone U1385-5 (11050 – 4500 cal yr B.P.) corresponds to the early to Middle Holocene.
406 This zone is marked by the expansion of TMF as well as the Mediterranean forest, reflecting
407 a regional increase in temperature and precipitation. Despite the low temporal resolution it is
408 consistent with nearby records with a maximum forest development at around 9000 cal yr B.
409 P. (Gomes et al., 2020). Minimum values of C_{29}/C_{31} ratio suggested a decrease in epicuticular
410 wax production by vegetation possibly do to the most favourable conditions for vegetation
411 development compared with the preceding zones. During this zone is noteworthy the warmer
412 SST around 18-20 °C.

413

414 **5. Discussion**

415 **[Figure 4], [Figure 5]**

416

417 **5.1. The effect of pCO₂ on biome changes during the LGM and deglaciation**

418

419 Whilst a classic interpretation of ecosystem dynamics as described for Site U1385 can be
420 proposed solely considering the variation of the main climatic parameters (temperature,



421 precipitation), we hypothesise that past changes in pCO₂ played an essential role in vegetation
422 change, specifically in the deglacial forest expansion. Here we re-evaluate the drivers of
423 vegetation change, explicitly considering the evolution of pCO₂ through the deglaciation. Our
424 discussion is informed by the present-day environmental and climatic space occupied by
425 different taxa in Portugal (Temperate Mediterranean forest – *Quercus* sp., Heathland -
426 Ericaceae family and semi-desertic taxa) (S.M. Fig. 2).

427

428 **LGM**

429

430 The pollen-based vegetation record from Site U1385 shows that during the LGM a grassland-
431 heathland mosaic dominated the landscape (Fig. 3d, e and Fig. 4d), a distinctive non-analogue
432 glacial vegetation cover. The prevalence of heath pollen in Iberian pollen records underpins
433 the classic view of the LGM in Iberia as a fairly humid interval, certainly compared with the
434 extreme aridity evident during Heinrich stadials (Naughton et al. 2007; Roucoux et al. 2005;
435 Sanchez-Goni et al. 2009; Combourieu-Nebout et al. 2009; Fletcher and Sanchez-Goni 2008).
436 Nevertheless the juxtaposition of high abundances of semi-desert and heathland taxa remains
437 intriguing. In terms of their present-day climatic space distribution, the STE and ERI taxa differ
438 in that the latter can occupy niches with high humidity, which contrasts with the arid-loving
439 conditions of the former (S.M. Fig. 2c). Interestingly, the environmental space for the
440 Ericaceae group (namely *Erica arborea*, *E. australis*, *Calluna vulgaris*) coincides with that
441 occupied by the *Quercus* genus, the main constituent of the TMF group (S.M. Fig. 2b). This
442 begs the question, if the environmental conditions that support heathland overlap with those
443 for *Quercus* sp., then why were forests not thriving during the LGM? The first answer could be
444 cold atmospheric temperatures, even if during the LGM the temperatures were not as extreme
445 as the ones observed during the HS1 (Bond et al., 1993; Rasmussen et al., 1996). As such a
446 potential controlling factor could be the low levels of pCO₂ during the LGM of between 180-
447 190 ppmv, which is amongst the lowest concentrations recorded during the history of land
448 plants (Pearson and Palmer, 2000; Tripathi et al., 2009). The global distribution of different
449 vegetation types as a function of temperature and precipitation was modelled under modern
450 and corrected for LGM CO₂ (185 ppm) showing qualitative differences in the distribution of
451 vegetation types (Shao et al., 2018). Under low pCO₂ grassland was favoured to the detriment
452 of evergreen broadleaf, evergreen and deciduous needle leaf forest. That study, however, did
453 not include ericaceous heathlands specifically, and it is not known whether this group has
454 adaptations permitting better functioning under low pCO₂ levels. We speculate that drought-
455 adapted traits in Mediterranean Ericaceae especially *E. arborea* including thick cuticles, small
456 leaf size, large photosynthetic thermal window and deep root system with large diameter and
457 a massive underground lignotuber (Gratani and Varone, 2004) may have been beneficial in
458 coping with the challenging trade-off between photosynthesis and water loss under very low
459 pCO₂. As such, the Ericaceae of the LGM may represent part of vegetation that coped well
460 with physiological constraints of the low pCO₂ world.

461 At the same time, we note that the LGM corresponds to a maximum in of the precession cycle,
462 which is recognised to promote a weakening of seasonal contrasts (reduced summer dryness)
463 and consistently associated with heathland development in the Iberian Peninsula (Fletcher
464 and Sanchez Goni, 2008; Sanchez Goni, 2008), in both glacials and interglacials (e.g. Oliveira
465 et al., 2017), including the Middle to Late Holocene (Gomes et al., 2020; Oliveira et al., 2018;
466 Chabaud et al., 2014). As such, during the LGM, the precession maximum promoting wetter
467 summers should have been a trigger for heathland development .



468 Diverse vegetation models have been used to understand the influence of climatic parameters
469 and pCO₂ during the LGM (e.g. Harrison and Prentice, 2003; Woillez et al., 2011; Shao et al.,
470 2018). There is a disagreement about the magnitude of the pCO₂ influence, from being
471 considered to have an equal influence (Izumi and Lezine, 2016) to being thought to be less
472 critical than climatic parameters (Woillez et al., 2011; Shao et al., 2018; Chen et al., 2019).
473 Harrison and Prentice (2003) also highlight models differences and the variable regional
474 expression of the influence of pCO₂ (with higher impact in tropical areas). However, these
475 studies agree that low pCO₂ had a negative physiological impact on forest development during
476 the LGM in different continents (Jolly and Haxeltine, 1997; Cowling, 1999; Harrison and
477 Prentice, 2003; Woillez et al., 2011; Shao et al., 2018; Chen et al., 2019). Jolly and Haxeltine
478 (1997) used BIOMOD to simulate LGM vs pre-industrial CO₂ levels under different climatic
479 conditions scenarios (temperature and precipitation) in tropical Africa; CO₂ was considered
480 the primary driver of biome change from tropical montane forests to shrubby heathland
481 ecosystems. This model included a photosynthetic scheme able to simulate plant response to
482 different levels of CO₂ and its impact on stomatal conductance and water stress. This study
483 showed that increasing pCO₂ (above ~190 ppmv), offsets the lower temperatures (changes of
484 -4 to -6 °C), allowing the forest to thrive and substitute heathland. However, plants with higher
485 climatic demands (temperature and precipitation), which is the case of most temperate trees,
486 are less competitive under low pCO₂ conditions, compared with evergreen microphyllous
487 species (e.g. *Erica* sp.). The ecological advantages of *Erica* sp. also include less demanding
488 edaphic requirements (low nutrient demand), more competitive re-sprouting strategy after
489 disturbance, especially fires, as well as a higher dispersal capacity compared with *Quercus*
490 sp. for example (Pausas, 2008).

491 The inclusion of pCO₂ in climatic reconstructions for LGM for Africa and Europe yields a wetter
492 LGM compared with reconstructions assuming pCO₂ present-day concentrations (Wu et al.,
493 2007). The implications of these experiments are important for the southwest Iberian region
494 and may help to resolve the apparent contradiction between vegetation (abundance of semi-
495 desertic plants and presence of heathland) and climate simulations which indicate enhanced
496 winter precipitation over southern Iberian and Northwest Africa due to southward shifting of
497 the wintertime westerlies (Beghin et al., 2016). In the absence of pCO₂ correction, temperature
498 could also be misinterpreted; the LGM vegetation for Mediterranean sites was simulated and
499 associated with warmer summer under LGM pCO₂, instead of the more cold conditions
500 simulated with present-day levels of CO₂ (Guiot et al., 2000). In Europe, pollen reconstruction
501 with steppe vegetation indicated warmer winter temperature for LGM pCO₂ compared with the
502 modern pCO₂ (Wu et al., 2007). The bias could extend to vegetation reconstructions; without
503 the pCO₂ effect, the cover of boreal and temperate forests is reduced, and evergreen forests
504 are overestimated for the LGM (Woillez et al., 2011).

505 Experiments determining plant thresholds in response to low pCO₂ have not received as much
506 attention as research on the impact of high pCO₂ levels (Gerhart and Ward, 2010; Dusenge
507 et al., 2019). When we assess the relationship between pCO₂, SST and TMF across the LGM
508 and deglaciation events we observe that LGM occurrence of TMF (i) corresponds to SSTs
509 below 15.5°C and pCO₂ below 225 ppmv and (ii) that values remain below 20% (Fig. 5). Within
510 African mountain environments, a value of 220 ppmv of pCO₂ has been suggested as a
511 threshold above which the forest could develop (Dupont et al., 2019). Therefore, we can infer
512 that the forest development in SW of Iberian during LGM may have been constrained by the
513 interaction of relatively low temperatures (with seasonal oscillations) and low levels of pCO₂
514 (~185 ppmv). One could speculate that a hypothetical increase of pCO₂, above 225 ppmv
515 values during the LGM would have permitted forest development in the southwest Iberian



516 Peninsula, although independent proxies for terrestrial temperatures and precipitation amount
517 are highly desirable.

518

519 **HS1**

520

521 During HS1, a Mediterranean steppe landscape with minimum arboreal development resulted
522 from the lowest temperatures and highest levels of aridity observed within the studied interval
523 (Fig. 3 and 5c). During this event, the potential effect of increasing pCO₂ (from ~185 to ~225
524 ppm) from 18.1 to ~16 cal ka B.P. (Fig. 3b) was not enough to counteract the limiting effect of
525 the climate conditions (coldest and driest atmospheric conditions), and indeed should have
526 exacerbated aridity stress at this time.. Regional models (Weather and Research Forecast
527 Model – WRF) reconstructing the potential vegetation with a pCO₂ correction show a reduction
528 in arboreal vegetation and increase of sparsely vegetated soil for the IP region during HS1
529 compared with the LGM (Ludwig et al., 2018). The reconstructed precipitation values for the
530 southwestern Iberian Peninsular (Tagus hydrographic basin catchment), show values below
531 700 mm/yr for HS1, which agrees with the pollen data and again the widespread semi-desertic
532 taxa development. Interestingly, the differences between HS1 and LGM are quite relevant,
533 which could explain the stronger development of the heathland in the LGM. The reconstructed
534 atmospheric temperature showed a longitudinal variation between the HS1 and LGM varying
535 from -2.5 to -1.5 °C; which are in line with the high percentages of semi-desertic taxa of Site
536 U1385, as well as other nearby IP records (Peñalba et al., 1997; Perez-Obiol and Julia, 1984;
537 Comborieu Nebout et al., 2002; Roucoux et al., 2005; Naughton et al., 2007; Fletcher and
538 Sánchez Goñi, 2008). Besides, the forest development was constrained across the territory,
539 and based on pollen data from marine and terrestrial records we do not observe any significant
540 (<5% TMF) latitudinal difference when comparing northern (e.g. Peñalba et al., 1997; Perez-
541 Obiol and Julia, 1984; Roucoux et al., 2005; Naughton et al., 2007) with southern (e.g. this
542 study; Comborieu Nebout et al., 2002; Fletcher and Sánchez Goñi, 2008) pollen records.
543 Furthermore, the relationship between pCO₂, SST and TMF across the HS1 show scattered
544 values of TMF (below 20%) occurring at temperatures below 15.5°C and pCO₂ below 225
545 ppmv (Fig. 5).

546

547 **BA**

548

549 The BA is characterised by favourable climatic conditions (higher temperatures, higher
550 moisture availability) for TMF development (Fig. 3c). The high temperature and a dry to wet
551 trend are likely the primary drivers of progressive forest development during the BA. However,
552 it is important also to consider a possible role of increasing of soil maturation (higher organic
553 matter content, pH, plant nutrients, during succession/development of this biome), as well as
554 a possible "fertilisation effect" of the stepwise increases of pCO₂ by ~15 ppmv around this time
555 interval (Fig. 3b). The simulations produced by BIOME3 for African Biomes (Tropical
556 forest/Ericaceous scrub) with a present climate showed that above 190 ppmv, the increase of
557 pCO₂ at intervals <20 ppmv, gradually offsets the negative effect of temperature changes;
558 above 250 ppmv with a maximum temperature change of ~-6°C the development of forest will
559 be promoted in detriment of the ericaceous scrubland (Jolly and Haxeltine, 1997).

560 The abrupt increases in pCO₂ at 16.3 Ka and 14.8 Ka (Marcott et al., 2014) (Fig. 3b), could
561 tentatively be associated with the slight increase of forest at the onset of the BA and with the
562 highest peaks of forest development observed during the BA (within age uncertainties of both
563 archives) (Fig. 3c). Cao et al. (2019), using pollen-based biome reconstruction, suggested that



564 worldwide expansion of forests was a consequence of the increasing pCO₂ superimposed
565 over the temperature increase between 21 ka and 14 ka. Cao et al. (2019) further emphasise
566 the role of CO₂ after the LGM driving a general northward expansion of forests and
567 replacement of grassland by temperate forests in Europe, by minimising moisture limitation
568 and enhancing WUE. Afterwards, from 14 ka to 9 ka, sufficient moisture (in a general
569 assumption) might also have played a significant role (Cao et al., 2019), whilst the higher levels
570 of pCO₂ may have been able to offset, at least at the end of the BA, the effect of any potential
571 reductions in moisture availability. During the BA, considering that temperature and moisture
572 availability was quasi-optimal, increases in pCO₂ levels (>225 ppmv) may have amplified TMF
573 expansion during this period (Fig. 4b and Fig. 5).

574

575 **YD**

576

577 The YD is characterised by a forest-grassland mosaic, as indicated by relatively high levels of
578 forest coexisting with semi-desertic taxa (Fig. 3c, d and Fig. 4a). Strong SST cooling (Fig. 3j)
579 may have been associated with cooler land surface temperatures. However, this impact may
580 have been offset by the positive effect of sufficient moisture availability (based on the presence
581 of TMF, Naughton et al. 2019) and the increasing trend of pCO₂ (Fig. 3b). Unfortunately, there
582 is a lack of independent precipitation proxies for this region, and Dennison et al. (2018)
583 highlight a lack of reliability in the speleothem proxies for precipitation in this region for this
584 time interval. We observe that the YD forest development occurs in association with similar
585 SSTs to those of the LGM and slightly higher than those of HS1. Meanwhile, pCO₂ was above
586 the 225 ppmv threshold throughout the YD, (reaching maximum values of ~260 ppmv, at ~12
587 Ka) (Fig. 5). The increase in pCO₂ may have enhanced plant productivity and WUE (Cowling
588 and Sykes, 1999; Ward et al., 2005) during the YD, partially compensating for the impact of
589 atmospheric cooling and drying. Schenk et al. (2018) suggest pCO₂ may play an essential role
590 in the forest development if enough moisture is available. It may be that the tree cover was
591 restricted to suitable, moist microhabitats and close to refuge zones, but was not as restricted
592 as in previous cold periods (Svenning et al., 2011), as pollen data also suggests (Fig. 3c).
593 Also, simulated data from vegetation-climate models based on pollen records for biome
594 reconstruction (Shao et al., 2018) and in a dynamic vegetation model (ORCHIDEE) driven by
595 outputs from an AOGCM (Wuillez et al., 2011) emphasise the influence of increasing pCO₂ as
596 a critical factor for worldwide forest development during the period including the YD (Shao et
597 al., 2018). Underlying these changes the increase in summer insolation (Fig. 3a), which
598 contributed to the increase of summer temperatures cannot be neglected as a promotor of
599 forest development, at least where trees were not excessively water-stressed. However
600 disentangling the isolated contribution of insolation vs pCO₂ requires sensitivity experiments,
601 not yet performed. In summary, the persistence of TMF during the YD, despite cold
602 temperatures with some seasonality, (warmer than the HS1), seems to be best explained by
603 the combined interaction between sufficient moisture availability, higher atmospheric
604 temperature, at least during summer (promoting forest development) and increasing pCO₂
605 (between ~245 and 265 ppmv) (Fig. 4a).

606

607 **5.2. C₂₉/C₃₁ ratio and C₃/C₄ dynamics: potentials and limitations**

608

609 Insights into the dominance of different plant physiological pathways can be potentially gained
610 using C₂₉/C₃₁ n-alkanes of Site U1385A (Fig. 3h). In general, C₂₉ and C₃₁, as well as other long-
611 chain alkanes with odd carbon numbers (e.g. C₂₉, C₃₁, C₃₃), are epicuticular waxes produced



612 by terrestrial plants, from which C_{29} could represent woody plants and C_{31} grasses (Meyers,
613 2003). However, caution in interpreting the C_{29}/C_{31} ratio in terms of taxonomic groups is
614 required since woody plants and grasses are both capable of producing C_{29} and C_{31} chain
615 lengths (Ortiz et al., 2010; Bush and McInerney, 2013). Furthermore, regional differences are
616 observed across the world and between biomes in terms of what long-chain n-alkanes a
617 species is producing (Bush and McInerney, 2013). Noting this limitation, the analysis of C_{29}/C_{31}
618 curve shows increasing values during the LGM to yield high values during the HS1, followed
619 by the YD underlying a decreasing trend towards the Holocene (Fig. 3h). The C_{29}/C_{31} is
620 positively: $r = 52\%$ (negatively: $r = -63\%$) correlated (Pearson's correlation coefficient) with the
621 semi-desertic (temperate Mediterranean forest) signals within this region over the same
622 interval (Fig. 3c, d and h). Therefore, we note that the anticipated general interpretation of the
623 C_{29}/C_{31} ratio as an indicator of the relative abundance of trees vs grasses does not hold for
624 our datasets (indeed the reverse is evident). Instead, we tentatively infer that C_{29}/C_{31} ratio in
625 this setting is expressing an adaptation of plants to aridity, and perhaps an increase in wind
626 strength conditions, which alter the moisture balance. The n-alkanes of leaf waxes are
627 produced to protect plants against the loss of water during the photosynthetic process (Post-
628 Beittenmiller, 1996; Jetter et al., 2006). We could expect that arid/cold conditions to be more
629 disturbing for woody plants than for grasses, as such the increase of the C_{29}/C_{31} during HS1
630 and YD, could suggest a climatic adaptation of woody plants by increasing the production of
631 leaf wax C_{29} . However, the traditional taxonomic generalisation of C_{29} woody versus C_{31}
632 grasses (Meyers, 2003), still needs some caution.

633 Other hypotheses to be explored and understood include the connection between the long-
634 chain n-alkanes and the dynamic between C_3 and C_4 plants. Nowadays, African savannahs
635 are dominated by C_4 plants, and biomarkers (including C_{31} n-alkanes) can be used to infer
636 their presence in past landscapes (Dupont et al., 2019). Worldwide, 80% of Poaceae (grasses)
637 and Cyperaceae (sedges) present a C_4 photosynthetic pathway (Sage, 2017) but with pollen
638 analysis, there is no confidence about the Poaceae and Cyperaceae pollen morphologic types
639 being exclusively or in its majority C_4 plants. We have grouped the Poaceae and the
640 Cyperaceae pollen taxa, noting the inherent limitations of this grouping (Fig. 3g). This group
641 (Poaceae + Cyperaceae) presents relatively high values with considerable oscillations
642 (potentially related to differences in time resolution) between the LGM and the BA and more
643 stable behaviour onwards. No particular correlation with other indicators (TMF or STE or
644 C_{29}/C_{31}) was evident, apart from the apparent instability before the Holocene. Interestingly,
645 within a laboratory setting, C_3 grasses are favoured in comparison with C_4 grasses, when
646 temperatures increase by 5 to 15°C with a pCO_2 of 200 ppm (Ehleringer et al., 1997; Edwards
647 et al., 2010). Furthermore, C_4 plants nowadays are mostly confined to the tropical grasslands
648 and savannahs; they are better adapted to environments with higher temperatures, aridity,
649 poor nutrient soils, and intensive disturbance caused by animals or fire regimes (Bond et al.,
650 2005; Edwards et al., 2010). Likewise, one should expect that in the Iberia after the LGM (Fig.
651 3 and 5) should be mainly composed by C_3 plants; considering the estimated SSTs indicating
652 relatively cold temperatures (Fig. 5) and the high percentages of *Artemisia* (C_3 plant) (S.M.
653 Fig. 1).

654 However, it is not currently possible to entirely rule out an increased importance of C_4 plants
655 in the glacial vegetation in the IP, because pollen morphology does not allow the separation
656 of these groups and biomarkers proxies have not been tested or reported to clarify the dynamic
657 between C_3/C_4 plants in the Temperate/Mediterranean biomes. The discrimination of C_3/C_4
658 grasses has been made on the basis of stable isotopes of ancient grass pollen (Nelson et al.,
659 2016) although the single grain isotopic measurements employed remain challenging to



660 implement. This highlights the theoretical possibility of the C₃/C₄ plant dynamic observed in
661 Africa (e.g. Dupont et al., 2019) and other savannahs ecosystems not being replicable (with
662 the current knowledge) in our study area. Biomarker species/groups fingerprinting studies are
663 required in order to eventually distinguish between C₃ and C₄ plants and then go onto exploring
664 the dynamics observed between C₃ and C₄, within IP-Mediterranean ecosystems during the
665 last deglaciation.

666 **6. Conclusion**

667

668 This study presents high-resolution pollen and SST records from Site U1385 which can be
669 used in future regional and global reconstructions and models, especially for the Iberian
670 Peninsula. A long-term analysis of climatic changes was comparable and consistent across
671 the Iberian records analysed, with the advantage of the new record having an average higher
672 resolution and a more robust radiocarbon chronology.

673 We explore the understanding of TMF dynamics under the influence of climatic change and
674 increasing pCO₂ throughout the LGM and deglaciation. Our analysis suggests that forest
675 development during the LGM may have been also constrained at least in part due to the low
676 pCO₂, acting as a modulator. The baseline climatic conditions to support heathland
677 development at present in the region are relatively similar to the ones required by some
678 *Quercus* sp, however, trees development benefits from more warmth months (Polunin and
679 Walters, 1984). During the LGM, the associated cold conditions and low seasonality together
680 with the exacerbation of drought stress resulting from the low concentration of pCO₂ might
681 have limited forest expansion. We speculate that certain traits of the Mediterranean Ericaceae,
682 including small leaf size, thick cuticular waxes and deep rooting which contribute to drought
683 tolerance at present may have promoted the development of heathlands during the LGM, as
684 previously observed in African uplands. During HS1, woody plant development was further
685 restricted by the impact of low temperatures as well aridity, under low pCO₂ and associated
686 with wider climatic perturbation evidenced in freshwater pulses. The BA characterises the
687 most suitable conditions for TMF development – warm, rising temperatures, moisture
688 availability, amplification of seasonality, and the increase of pCO₂. The TMF persistence, and
689 the forest–grassland mosaic, during the YD, can be best explained by the joint imprint of
690 moisture availability and higher pCO₂. The role of pCO₂ was, in our opinion, fundamental for
691 the significant TMF development during the late glacial in southwestern Iberia, by comparison
692 with precedent cold intervals (LGM and HS1). Although other co-hypotheses must be better
693 assessed, ideally against future development of independent (non-vegetation) proxies for
694 precipitation and temperature during this time-slice, so far there are no regional
695 reconstructions that consider the co-effect of moisture and pCO₂.

696 Considering the response of TMF and xerophytic taxa in our pollen record, we consider the
697 pCO₂ value of ~225 ppm as a critical limit for forest expansion in the IP during the last
698 deglaciation. This hypothesis should be explored through model simulations to establish the
699 amplitude and critical thresholds of pCO₂ impacts on regional vegetation, as well as, in past
700 cold periods.

701 The relation of C₃ and C₄ plants in the Mediterranean domain needs further attention since the
702 long-chain *n*-alkanes do not yet provide a reliable picture to disentangle the dynamic between
703 woody plants and grasses. We applied a biomarker proxy C₂₉/C₃₁ which is positively correlated
704 with the semi-desertic pollen curve and negatively with TMF. This points to its potential as a
705 proxy of aridity, testifying the increase of leaf-wax C₂₉ production during the dry periods, albeit
706 in a regionally-specific way, and noting that this is not in agreement with previous inferences



707 regarding the discrimination of herbaceous and arboreal taxa. Another suggestion is to test
708 the C_{29}/C_{31} ratio for other periods in the past, throughout glacial periods.
709 Many global-scale LGM and deglacial reconstructions have been undertaken with a
710 preferential focus on the LGM and YD. An enhanced effort by the modelling community in
711 developing transient regional simulations covering the last deglaciation may be valuable, to
712 allow a more precise comparison/testing with proxy data. Our new data and regional pollen
713 synthesis provide a good target for modelling. Furthermore, this study can provide a baseline
714 understanding and essential context (potential analogue) for present-day world changes in
715 arid and semi-arid ecosystems in terms of their potential future evolution under rapidly
716 changing pCO_2 .

717

718 **Author contribution**

719

720 SDG, WF, FN and AS contributed to the conception and design of the study, data analysis
721 and interpretation. Also they were responsible for the grant application to NERC. SDG
722 performed pollen analysis. TR performed biomarkers analysis. AR performed assemblage
723 foraminifers picking for radiocarbon dating and draw figure 1. SDG prepared the original draft
724 and wrote the manuscript including figures with the critical input (edition and revision) from all
725 co-authors.

726

727 **Competing interests**

728

729 The authors declare that they have no conflict of interest.

730

731 **Acknowledgements**

732

733 This research was supported by the Portuguese Foundation for Science and Technology
734 (FCT) SFRH/BD/128984/2017 PhD grant to SDG, the ULImATum (IF/01489/2015) and, the
735 Hydrosifts (PTDC/CTA-CLI/4297/2021) projects; CCMAR FCT Research Unit - project
736 UIDB/04326/2020, CCMAR BCC grant (Incentivo/MAR/LA00015/2014) to FN, FCT contract
737 (CEECIND/02208/2017) to DO, WarmWorld Project (PTDC/CTA-GEO/29897/2017) for
738 Biomarker analyses, and grant (SFRH/BPD/108600/2015) to TR. The six radiocarbon dates
739 were obtained through the NERC radiocarbon application award NERC 2136.1018. The
740 contributions of L. Devaux are gratefully acknowledged (Bordeaux 1 University, EPOC, UMR-
741 CNRS 5805) for his assistance in palynological treatments.

742

743

744

745 **References**

746

- 747 Allen, J.R., Huntley, B., and Watts, W.A.: The vegetation and climate of northwest Iberia over
748 the last 14,000 years, *J Quaternary Sci.*, 11,125-147, [https://doi.org/10.1002/\(SICI\)1099-1417\(199603/04\)11:2<125::AID-JQS232>3.0.CO;2-U](https://doi.org/10.1002/(SICI)1099-1417(199603/04)11:2<125::AID-JQS232>3.0.CO;2-U), 1996.
750 Alley, R.B. and Clark, P.U.: The deglaciation of the northern hemisphere: a global perspective,
751 *Annu Rev Earth Pl Sc*, 27, 149-182, <https://doi.org/10.1146/annurev.earth.27.1.149>, 1999.
752 Aranbarri, J., González-Sampériz, P., Valero-Garcés, B., Moreno, A., Gil-Romera, G., Sevilla-
753 Callejo, M., García-Prieto, E., Di Rita, F., Mata, M.P., Morellón, M., and Magri, D.: Rapid



- 754 climatic changes and resilient vegetation during the Lateglacial and Holocene in a
755 continental region of south-western Europe, *Global Planet. Change*, 114, 50-65,
756 <https://doi.org/10.1016/j.gloplacha.2014.01.003>, 2014.
- 757 Ausín, B., Hodell, D.A., Cutmore, A., and Eglinton, T.I.: The impact of abrupt deglacial climate
758 variability on productivity and upwelling on the southwestern Iberian margin, *Quaternary*
759 *Sci. Rev.*, 230, 106-139, <https://doi.org/10.1016/j.quascirev.2019.106139>, 2020.
- 760 Bard, E., Arnold, M., Maurice, P., Duprat, J., Moyes, J., and Duplessy, J.C.: Retreat velocity
761 of the North Atlantic polar front during the last deglaciation determined by ¹⁴C accelerator
762 mass spectrometry, *Nature*, 328, 791, <https://doi.org/10.1038/328791a0>, 1987.
- 763 Bard, E., Ménot, G., Rostek, F., Licari, L., Böning, P., Edwards, R.L., Cheng, H., Wang, Y.,
764 and Heaton, T.J.: Radiocarbon calibration/comparison records based on marine sediments
765 from the Pakistan and Iberian margins, *Radiocarbon*, 55, 1999-2019, [https://doi-
766 org.manchester.idm.oclc.org/10.2458/azu_js_rc.55.17114](https://doi-org.manchester.idm.oclc.org/10.2458/azu_js_rc.55.17114), 2013.
- 767 Bard, E., Ménot-Combes, G., and Rostek, F.: Present status of radiocarbon calibration and
768 comparison records based on Polynesian corals and Iberian Margin sediments,
769 *Radiocarbon*, 46, 1189-202, <https://doi.org/10.1017/S0033822200033087>, 2004a.
- 770 Bard, E., Rostek, F., and Ménot-Combes, G.: Radiocarbon calibration beyond 20,000 ¹⁴C yr
771 B.P. by means of planktonic foraminifera of the Iberian Margin, *Quaternary Res.*, 61, 204-
772 14, <https://doi.org/10.1016/j.yqres.2003.11.006>, 2004b.
- 773 Bard, E., Rostek, F., Turon, J.L., and Gendreau, S.: Hydrological impact of Heinrich events in
774 the subtropical northeast Atlantic, *Science*, 289, 1321-1324,
775 [10.1126/science.289.5483.1321](https://doi.org/10.1126/science.289.5483.1321), 2000.
- 776 Bartlein, P.J., Harrison, S.P., Brewer, S., Connor, S., Davis, B.A., Gajewski, K., Guiot, J.,
777 Harrison-Prentice, T.I., Henderson, A., Peyron, O., and Prentice, I.C.: Pollen-based
778 continental climate reconstructions at 6 and 21 ka: a global synthesis, *Clim. Dynam.*, 37,
779 775-802, <https://doi.org/10.1007/s00382-010-0904-1>, 2011.
- 780 Beghin, P., Charbit, S., Kageyama, M., Combourieu-Nebout, N., Hatté, C., Dumas, C., and
781 Peterschmitt, J.-Y.: What drives LGM precipitation over the western Mediterranean? A
782 study focused on the Iberian Peninsula and northern Morocco, *Clim. Dynam.*, 46, 2611-
783 2631, <https://doi.org/10.1007/s00382-015-2720-0>, 2016.
- 784 Bennet et al 2009 CONISS
- 785 Bennett, K.D.: Documentation for psimpoll 4.27 and pscomb 1.03: C programs for plotting and
786 analysing pollen data, <http://www.chrono.qub.ac.uk/psimpoll/psimpoll.html>, last access 14
787 January 2020.
- 788 Blaauw, M. and Christen, J.A.: Flexible paleoclimate age-depth models using an
789 autoregressive gamma process, *Bayesian Anal.*, 6, 457-474, [10.1214/ba/1339616472](https://doi.org/10.1214/ba/1339616472),
790 2011.
- 791 Boessenkool, K. P., Brinkhuis, H., Schönfeld, J., and Targarona, J.: North Atlantic sea-surface
792 temperature changes and the climate of western Iberia during the last deglaciation; a
793 marine palynological approach, *Global Planet. Change*, 30, 33-39, [10.1016/S0921-
794 8181\(01\)00075-3](https://doi.org/10.1016/S0921-8181(01)00075-3), 2001.
- 795 Bond, W.J., Woodward, F.I. and Midgley, G.F.: The global distribution of ecosystems in a
796 world without fire, *New phytologist*, 165, 525-538, [https://doi.org/10.1111/j.1469-
797 8137.2004.01252.x](https://doi.org/10.1111/j.1469-8137.2004.01252.x), 2005
- 798 Brassell, S.C., Eglinton, G., Marlowe, I.T., Pflaumann, U., and Sarnthein, M.: Molecular
799 stratigraphy: a new tool for climatic assessment, *Nature*, 320, 129-133,
800 <https://doi.org/10.1038/320129a0>, 1986.



- 801 Bush, R.T. and McInerney, F.A.: Leaf wax n-alkane distributions in and across modern plants:
802 implications for paleoecology and chemotaxonomy, *Geochim. Cosmochim. Ac.*, 117, 161-
803 179, 2013.
- 804 Camuera, J., Jiménez-Moreno, G., Ramos-Román, M.J., García-Alix, A., Toney, J.L.,
805 Anderson, R.S., Jiménez-Espejo, F., Bright, J., Webster, C., Yanes, Y., and Carrión, J.S.:
806 Vegetation and climate changes during the last two glacial-interglacial cycles in the western
807 Mediterranean: A new long pollen record from Padul (southern Iberian Peninsula),
808 *Quaternary Sci. Rev.*, 205, 86-105, <https://doi.org/10.1016/j.quascirev.2018.12.013>, 2019.
- 809 Cao, X., Tian, F., Dallmeyer, A., and Herzschuh, U.: Northern Hemisphere biome changes (>
810 30° N) since 40 cal ka B.P. and their driving factors inferred from model-data
811 comparisons, *Quaternary Sci. Rev.*, 220, 291-309,
812 <https://doi.org/10.1016/j.quascirev.2019.07.034>, 2019.
- 813 Carrión, J.S.: Patterns and processes of Late Quaternary environmental change in a montane
814 region of southwestern Europe, *Quaternary Sci. Rev.*, 21, 2047-2066. 10.1016/S0277-
815 3791(02)00010-0, 2002.
- 816 Chabaud, L., Sánchez Goñi, M.F., Desprat, S., and Rossignol, L.: Land-sea climatic variability
817 in the eastern North Atlantic subtropical region over the last 14,200 years: Atmospheric and
818 oceanic processes at different timescales, *The Holocene*, 24, 787-797,
819 <https://doi.org/10.1177/0959683614530439>, 2014.
- 820 Chen, W., Zhu, D., Ciais, P., Huang, C., Viovy, N., and Kageyama, M.: Response of vegetation
821 cover to CO₂ and climate changes between Last Glacial Maximum and pre-industrial
822 period in a dynamic global vegetation model, *Quaternary Sci. Rev.*, 218, 293-305,
823 <https://doi.org/10.1016/j.quascirev.2019.06.003>, 2019.
- 824 Clark, P.U., Shakun, J.D., Baker, P.A., Bartlein, P.J., Brewer, S., Brook, E., Carlson, A.E.,
825 Cheng, H., Kaufman, D.S., Liu, Z., and Marchitto, T.M.: Global climate evolution during the
826 last deglaciation. *P. Natl. Acad. Sci. USA*, 109, E1134-E1142,
827 <https://doi.org/10.1073/pnas.1116619109>, 2012
- 828 Claussen, M., Selent, K., Brovkin, V., Raddatz, T., and Gayler, V.: Impact of CO₂ and climate
829 on Last Glacial Maximum vegetation - A factor separation, *Biogeosciences*, 10, 3593-3604,
830 10.5194/bg-10-3593-2013, 2013.
- 831 Cleator, S.F., Harrison, S.P., Nichols, N.K., Prentice, I.C., and Roulstone, I.: A new
832 multivariable benchmark for Last Glacial Maximum climate simulations. *Clim. Past*, 16, 699-
833 712, <https://doi.org/10.5194/cp-16-699-2020>, 2020.
- 834 Combourieu Nebout, N., Peyron, O., Dormoy, I., Desprat, S., Beaudouin, C., Kotthoff, U., and
835 Marret, F.: Rapid climatic variability in the west Mediterranean during the last 25 000 years
836 from high resolution pollen data, *Clim. Past*, 5, 503-521, [https://doi.org/10.5194/cp-5-503-](https://doi.org/10.5194/cp-5-503-2009)
837 2009, 2009.
- 838 Combourieu Nebout, N., Turon, J.L., Zahn, R., Capotondi, L., Londeix, L., and Pahnke, K.:
839 Enhanced aridity and atmospheric high-pressure stability over the western Mediterranean
840 during the North Atlantic cold events of the past 50 k.y., *Geology*, 30,
841 [https://doi.org/10.1130/0091-7613\(2002\)030<0863:EAAAHP>2.0.CO;2](https://doi.org/10.1130/0091-7613(2002)030<0863:EAAAHP>2.0.CO;2), 2002.
- 842 Combourieu-Nebout, N., Paterne, M., Turon, J.L., and Siani, G.: A high-resolution record of
843 the last deglaciation in the central Mediterranean Sea: Palaeovegetation and
844 palaeohydrological evolution, *Quaternary Sci. Rev.*, 17, 303-317,
845 [https://doi.org/10.1016/S0277-3791\(97\)00039-5](https://doi.org/10.1016/S0277-3791(97)00039-5), 1998.
- 846 Cowling, S.A. and Sykes, M.T.: Physiological significance of low atmospheric CO₂ for plant-
847 climate interactions, *Quaternary Res.*, 52, 237-242,
848 <https://doi.org/10.1006/qres.1999.2065>, 1999.



- 849 Cowling, S.A.: Simulated effects of low atmospheric CO₂ on structure and composition of
850 North American vegetation at the Last Glacial Maximum, *Global Ecol. Biogeogr.*, 8, 81-93,
851 <https://doi.org/10.1046/j.1365-2699.1999.00136.x>, 1999.
- 852 Cramer, W., Bondeau, A., Woodward, F.I., Prentice, I.C., Betts, R.A., Brovkin, V., Cox, P.M.,
853 Fisher, V., Foley, J.A., Friend, A.D., and Kucharik, C.: Global response of terrestrial
854 ecosystem structure and function to CO₂ and climate change: results from six dynamic
855 global vegetation models, *Glob. Change Biol.*, 7, 357-373, <https://doi.org/10.1046/j.1365-2486.2001.00383.x>, 2001.
- 857 Cranwell, P.A.: Chain-length distribution of n-alkanes from lake sediments in relation to post-
858 glacial environmental change, *Freshwater Biology*, 3, 259-265,
859 <https://doi.org/10.1111/j.1365-2427.1973.tb00921.x>, 1973.
- 860 Crucifix, M., Braconnot, P., Harrison, S.P., and Otto-Bliesner, B.: Second phase of
861 paleoclimate modelling intercomparison project, *EOS T. Am. Geophys. Un.*, 86, 264-264,
862 <https://doi.org/10.1029/2005EO280003>, 2005.
- 863 Denniston, R.F., Houts, A.N., Asmerom, Y., Wanamaker Jr, A.D., Haws, J.A., Polyak, V.J.,
864 Thatcher, D.L., Altan-Ochir, S., Borowske, A.C., Breitenbach, S.F. and Ummenhofer, C.C.,
865 2018. A stalagmite test of North Atlantic SST and Iberian hydroclimate linkages over the
866 last two glacial cycles. *Climate of the Past*, 14. Doi: 10.5194/cp-14-1893-2018
- 867 Denton, G.H., Anderson, R.F., Toggweiler, J.R., Edwards, R.L., Schaefer, J.M., and Putnam,
868 A.E.: The last glacial termination, *Science*, 328, 1652-1656, [10.1126/science.1184119](https://doi.org/10.1126/science.1184119),
869 2010.
- 870 Dormoy, I., Peyron, O., Combourieu Nebout, N., Goring, S., Kotthoff, U., Magny, M., and
871 Pross, J.: Terrestrial climate variability and seasonality changes in the Mediterranean
872 region between 15 000 and 4000 years BP deduced from marine pollen records, *Clim.*
873 *Past*, 5, 615-632, <https://doi.org/10.5194/cp-5-615-2009>, 2009.
- 874 Dupont, L.M., Caley, T., and Castañeda, I.S.: Effects of atmospheric CO₂ variability of the
875 past 800 kyr on the biomes of southeast Africa, *Clim. Past*, 15, 1083-1097,
876 <https://doi.org/10.5194/cp-15-1083-2019>.
- 877 Dusenge, M.E., Duarte, A.G., and Way, D.A.: Plant carbon metabolism and climate change:
878 elevated CO₂ and temperature impacts on photosynthesis, photorespiration and
879 respiration, *New Phytologist*, 221, 32-49, <https://doi.org/10.1111/nph.15283>, 2019.
- 880 Edwards, E.J., Osborne, C.P., Strömberg, C.A., Smith, S.A. and C4 Grasses Consortium: The
881 origins of C4 grasslands: integrating evolutionary and ecosystem science, *Science*, 328,
882 587-591, <https://doi.org/10.1126/science.1177216>, 2010.
- 883 Ehleringer, J.R., Cerling, T.E., and Helliker, B.R.: C4 photosynthesis, atmospheric CO₂, and
884 climate, *Oecologia*, 112, 285-299, 1997.
- 885 Elenga, H., Peyron, O., Bonnefille, R., Jolly, D., Cheddadi, R., Guiot, J., Andrieu, V., Bottema,
886 S., Buchet, G., De Beaulieu, J.L., and Hamilton, A.C.: Pollen-based biome reconstruction
887 for southern Europe and Africa 18,000 yr BP, *J. Biogeogr.*, 27, 621-634,
888 <https://doi.org/10.1046/j.1365-2699.2000.00430.x>, 2000.
- 889 Faegri, K., Kaland, P.E. and Krzywinski, K., *Textbook of pollen analysis*, 4th Edition, John Wiley
890 & Sons Ltd., Chichester, 1989.
- 891 Farquhar, G.D. and Lloyd, J.: Carbon and Oxygen Isotope Effects in the Exchange of Carbon
892 Dioxide between Terrestrial Plants and the Atmosphere, in: *Stable Isotopes and Plant*
893 *Carbon/Water Relations*, edited by: Ehleringer, J.R., Hall, A.E., and Farquhar, G.D.,
894 Academic Press, New York, 47-70, <https://doi.org/10.1016/C2009-0-03312-1>, 1993.



- 895 Fletcher, W.J. and Sánchez Goñi, M.F.: Orbital-and sub-orbital-scale climate impacts on
896 vegetation of the western Mediterranean basin over the last 48,000 yr, *Quaternary Res.*,
897 70, 451-464, <https://doi.org/10.1016/j.yqres.2008.07.002>, 2008.
- 898 Fletcher, W.J., Goñi, M.S., Peyron, O., and Dormoy, I.: Abrupt climate changes of the last
899 deglaciation detected in a Western Mediterranean forest record, *Clim. Past*, 6, 245-264,
900 <https://doi.org/10.5194/cp-6-245-2010>, 2010a.
- 901 Fletcher, W.J., Sánchez Goñi, M.F., Allen, J.R.M., Cheddadi, R., Combourieu-Nebout, N.,
902 Huntley, B., Lawson, I., Londeix, L., Magri, D., Margari, V., Müller, U.C., Naughton, F.,
903 Novenko, E., Roucoux, K., Tzedakis, P.C.: Millennial-scale variability during the last glacial
904 in vegetation records from Europe, *Quat. Sci. Rev.* 29, 2839-2864,
905 <https://doi.org/10.1016/j.quascirev.2009.11.015>, 2010b.
- 906 Gerhart, L.M. and Ward, J.K.: Plant responses to low [CO₂] of the past, *New Phytol.*, 188, 674-
907 695, <https://doi.org/10.1111/j.1469-8137.2010.03441.x>, 2010.
- 908 Gomes, S.D., Fletcher, W.J., Rodrigues, T., Stone, A., Abrantes, F., and Naughton, F.: Time-
909 transgressive Holocene maximum of temperate and Mediterranean forest development
910 across the Iberian Peninsula reflects orbital forcing, *Palaeogeogr. Palaeoclimatol.*, 550, 109739,
911 <https://doi.org/10.1016/j.palaeo.2020.109739>, 2020.
- 912 Gratani, L. and Varone, L.: Leaf key traits of *Erica arborea* L., *Erica multiflora* L. and
913 *Rosmarinus officinalis* L. co-occurring in the Mediterranean maquis. *Flora-Morphology,*
914 *Distribution, Functional Ecology of Plants*, 199, 58-69, [https://doi.org/10.1078/0367-2530-](https://doi.org/10.1078/0367-2530-00130)
915 00130, 2004.
- 916 Grimalt, J. O., Calvo, E., and Pelejero, C.: Sea surface paleotemperature errors in U^k37
917 estimation due to alkenone measurements near the limit of detection, *Paleoceanography*,
918 16, 226-232, [10.1029/1999PA000440](https://doi.org/10.1029/1999PA000440), 2001.
- 919 Guiot, J., Torre, F., Jolly, D., Peyron, O., Boreux, J.J., and Cheddadi, R.: Inverse vegetation
920 modeling by Monte Carlo sampling to reconstruct palaeoclimates under changed
921 precipitation seasonality and CO₂ conditions: application to glacial climate in
922 Mediterranean region, *Ecol. Model.*, 127, 119-140, [https://doi.org/10.1016/S0304-](https://doi.org/10.1016/S0304-3800(99)00219-7)
923 3800(99)00219-7, 2000.
- 924 Harrison, S. P., Bartlein, P. J., and Prentice, I. C.: What have we learnt from palaeoclimate
925 simulations?, *J. Quaternary Sci.*, 314, 363-385, <https://doi.org/10.1002/jqs.2842>, 2016.
- 926 Harrison, S.P. and Prentice, C.I.: Climate and CO₂ controls on global vegetation distribution
927 at the last glacial maximum: analysis based on palaeovegetation data, biome modelling
928 and palaeoclimate simulations, *Glob. Chang. Biol.*, 9, 983-1004,
929 <https://doi.org/10.1046/j.1365-2486.2003.00640.x>, 2003.
- 930 Heusser, L. and Balsam, W.L.: Pollen distribution in the northeast Pacific Ocean, *Quaternary*
931 *Res.*, 7, 45-62, [https://doi.org/10.1016/0033-5894\(77\)90013-8](https://doi.org/10.1016/0033-5894(77)90013-8), 1977.
- 932 Hodell, D., Lourens, L., Crowhurst, S., Konijnendijk, T., Tjallingii, R., Jiménez-Espejo, F.,
933 Skinner, L., Tzedakis, P.C., Members, T.S.S.P., Abrantes, F., and Acton, G.D.: A reference
934 time scale for Site U1385 (Shackleton Site) on the SW Iberian Margin, *Global and Planet.*
935 *Change*, 133, 49-64, <https://doi.org/10.1016/j.gloplacha.2015.07.002>, 2015.
- 936 Huang, J.G., Bergeron, Y., Denneler, B., Berninger, F., and Tardif, J.: Response of forest trees
937 to increased atmospheric CO₂, *Critical Reviews in Plant Sciences*, 26, 265-283, 2007.
- 938 Izumi, K. and Lézine, A.M.: Pollen-based biome reconstructions over the past 18,000 years
939 and atmospheric CO₂ impacts on vegetation in equatorial mountains of Africa, *Quat. Sci.*
940 *Rev.*, 152, 93-103, <https://dx.doi.org/10.1016/j.quascirev.2016.09.023>, 2016.



- 941 Jetter, R., Kunst, L., and Samuels, A.L.: Composition of plant cuticular waxes, in: *Biology of*
942 *the Plant Cuticle*, Annual Plant Reviews, edited by: Riederer, M., Müller, C., Blackwell,
943 Oxford, 145-181, <https://doi.org/10.1002/9780470988718.ch4>, 2006.
- 944 Jolly, D. and Haxeltine, A.: Effect of Low Glacial Atmospheric CO₂ on Tropical African Montane
945 Vegetation, *Science*, 276, 786-788, <https://doi.org/10.1126/SCIENCE.276.5313.786>, 1997.
- 946 Körner, C.: Biosphere responses to CO₂ enrichment, *Ecol. Appl.*, 10, 1590-
947 1619, [https://doi.org/10.1890/1051-0761\(2000\)010\[1590: BRTCE\]2.0.CO;2](https://doi.org/10.1890/1051-0761(2000)010[1590: BRTCE]2.0.CO;2), 2000.
- 948 Ludwig, P., Shao, Y., Kehl, M., and Weniger, G.-C.: The Last Glacial Maximum and Heinrich
949 event I on the Iberian Peninsula: A regional climate modelling study for understanding
950 human settlement patterns, *Glob. Planet. Change*, 170, 34-47,
951 <https://doi.org/10.1016/J.GLOPLACHA.2018.08.006>, 2018.
- 952 Lynch-Stieglitz, J., Adkins, J.F., Curry, W.B., Dokken, T., Hall, I.R., Herguera, J.C., Hirschi,
953 J.J.M., Ivanova, E.V., Kissel, C., Marchal, O., and Marchitto, T.M.: Atlantic meridional
954 overturning circulation during the last glacial maximum, *Science*, 316, 66-69,
955 <https://doi.org/10.1126/science.1137127>, 2007.
- 956 Marcott, S.A., Bauska, T.K., Buizert, C., Steig, E.J., Rosen, J.L., Cuffey, K.M., Fudge, T.J.,
957 Severinghaus, J.P., Ahn, J., Kalk, M.L., McConnell, J.R., Sowers, T., Taylor, K.C., White,
958 J.W.C., Brook, E.J.: Centennial-scale changes in the global carbon cycle during the last
959 deglaciation, *Nature*, 514, 616-619, <https://doi.org/10.1038/nature13799>, 2014.
- 960 Martrat, B., Grimalt, J. O., Shackleton, N. J., de Abreu, L., Hutterli, M. A., and Stocker, T. F.:
961 Four climate cycles of recurring deep and surface water destabilisations on the Iberian
962 margin, *Science*, 317, 502 - 507, <https://doi.org/10.1126/science.1139994>, 2007.
- 963 Martrat, B., Jimenez-Amat, P., Zahn, R., and Grimalt, J.O.: Similarities and dissimilarities
964 between the last two deglaciations and interglaciations in the North Atlantic region,
965 *Quaternary Sci. Rev.*, 99, 122-134, <https://doi.org/10.1016/j.quascirev.2014.06.016>, 2014.
- 966 McAndrews, J.H. and King, J.E.: Pollen of the North American Quaternary: the top twenty,
967 *Geoscience and Man*, 15, 41-49, <https://doi.org/10.2307/3687256>, 1976.
- 968 Meyers, P.A.: Applications of organic geochemistry to paleolimnological reconstructions: a
969 summary of examples from the Laurentian Great Lakes, *Org. Geochem.*, 34, 261-289,
970 [https://doi.org/10.1016/S0146-6380\(02\)00168-7](https://doi.org/10.1016/S0146-6380(02)00168-7), 2003.
- 971 Monnin, E., Indermühle, A., Dällenbach, A., Flückiger, J., Stauffer, B., Stocker, T.F., Raynaud,
972 D., Barnola, J.M.: Atmospheric CO₂ concentrations over the last glacial termination,
973 *Science*, 291, 112-114, <https://doi.org/10.1126/science.291.5501.112>, 2001.
- 974 Moore, P.D., Webb, J.A. and Collison, M.E.: *Pollen analysis*. Blackwell scientific publications,
975 Oxford, 1991.
- 976 Morales-Molino, C. and García-Antón, M.: Vegetation and fire history since the last glacial
977 maximum in an inland area of the western Mediterranean Basin (Northern Iberian Plateau,
978 NW Spain), *Quaternary Res.*, 81, 63-77, <https://doi.org/10.1016/j.yqres.2013.10.010>, 2014.
- 979 Morales-Molino, C., Devaux, L., Georget, M., Hanquiez, V., and Goñi, M.F.S.: Modern pollen
980 representation of the vegetation of the Tagus Basin (central Iberian Peninsula), *Rev.*
981 *Palaeobot. Palyno.*, 276, 104193, <https://doi.org/10.1016/j.revpalbo.2020.104193>, 2020.
- 982 Müller, P., Kirst, G., Ruhland, G., Storch, I.V., Rosell-Melé, A.: Calibration of the alkenone
983 index U^k₃₇ based on core-tops the eastern South Atlantic and global ocean (60°N-60°S),
984 *Geochim. Cosmochim. Ac.*, 62, 1757-1772, [https://doi.org/10.1016/S0016-7037\(98\)00097-](https://doi.org/10.1016/S0016-7037(98)00097-0)
985 0, 1998.
- 986 Naughton, F., Costas, S., Gomes, S.D., Desprat, S., Rodrigues, T., Goñi, M.S., Renssen, H.,
987 Trigo, R., Bronk-Ramsey, C., Oliveira, D., and Salgueiro, E.: Coupled ocean and



- 988 atmospheric changes during Greenland stadial 1 in southwestern Europe, *Quaternary Sci.*
989 *Rev.*, 212, 108-120, <https://doi.org/10.1016/j.quascirev.2019.03.033>, 2019.
- 990 Naughton, F., Drago, T., Sanchez-Goñi, M.F., and Freitas, M.C.: Climate variability in the
991 North-Western Iberian Peninsula during the last deglaciation, in: *Oceans and the*
992 *atmospheric carbon content*, edited by: Duarte, P., Santana-Casiano, M., Springer,
993 Dordrecht, 1-22, 2011.
- 994 Naughton, F., Goñi, M.S., Desprat, S., Turon, J.L., Duprat, J., Malaizé, B., Joli, C., Cortijo, E.,
995 Drago, T., and Freitas, M.C.: Present-day and past (last 25 000 years) marine pollen signal
996 off western Iberia, *Marine Micropaleontology*, 62, 91-114,
997 [10.1016/j.marmicro.2006.07.006](https://doi.org/10.1016/j.marmicro.2006.07.006), 2007.
- 998 Naughton, F., Sánchez Goñi, M.S., Rodrigues, T., Salgueiro, E., Costas, S., Desprat, S.,
999 Duprat, J., Michel, E., Rossignol, L., Zaragosi, S., and Voelker, A.H.L.: Climate variability
1000 across the last deglaciation in NW Iberia and its margin, *Quaternary Int.*, 414, 9-22,
1001 <https://doi.org/10.1016/j.quaint.2015.08.073>, 2016.
- 1002 Nelson, D.M., Urban, M.A., Kershaw, A.P., and Hu, F.S.: Late-Quaternary variation in C3 and
1003 C4 grass abundance in southeastern Australia as inferred from $\delta^{13}\text{C}$ analysis: Assessing
1004 the roles of climate, pCO₂, and fire, *Quaternary Sci. Rev.*, 139, 67-76,
1005 <https://doi.org/10.1016/j.quascirev.2016.03.006>, 2016.
- 1006 Oliveira, D., Desprat, S., Yin, Q., Naughton, F., Trigo, R., Rodrigues, T., Abrantes, F., and
1007 Sánchez Goñi, M.F.: Unraveling the forcings controlling the vegetation and climate of the
1008 best orbital analogues for the present interglacial in SW Europe, *Clim. Dynam.*, 51, 667-
1009 686, <https://doi.org/10.1007/s00382-017-3948-7>, 2018.
- 1010 Ortiz, J.E., Torres, T., Delgado, A., Llamas, J.F., Soler, V., Valle, M., Julià, R., Moreno, L., and
1011 Díaz-Bautista, A.: Palaeoenvironmental changes in the Padul Basin (Granada, Spain) over
1012 the last 1 Ma based on the biomarker content, *Palaeogeogr. Palaeoclimatol.*, 298, 286-299,
1013 <https://doi.org/10.1016/j.palaeo.2010.10.003>, 2010.
- 1014 Pausas, J.G., Llovet, J., Rodrigo, A., and Vallejo, R.: Are wildfires a disaster in the
1015 Mediterranean basin? – A review, *International Journal of wildland fire*, 17, 713-723,
1016 <https://doi.org/10.1071/WF07151>, 2009.
- 1017 Pearson, P.N. and Palmer, M.R.: Atmospheric carbon dioxide concentrations over the past 60
1018 million years, *Nature*, 406, 695-699, <https://doi.org/10.1038/35021000>, 2000.
- 1019 Peñalba, M.C., Arnold, M., Guiot, J., Duplessy, J.C., Beaulieu, J.-L.: Termination of the last
1020 glaciation in the Iberian Peninsula inferred from the pollen sequence of Quintanar de la
1021 Sierra, *Quaternary Res.*, 48, 205-214, <https://doi.org/10.1006/qres.1997.1922>, 1997.
- 1022 Pèrez-Obiol, R. and Julià, R.: Climatic change on the Iberian Peninsula recorded in a 30,000-
1023 yr pollen record from Lake Banyoles, *Quaternary Res.*, 41, 91-98,
1024 <https://doi.org/10.1006/qres.1994.1010>, 1994.
- 1025 Peyron, O., Guiot, J., Cheddadi, R., Tarasov, P., Reille, M., de Beaulieu, J.L., Bottema, S.,
1026 and Andrieu, V.: Climatic reconstruction in Europe for 18,000 yr BP from pollen data,
1027 *Quaternary Res.*, 49, 183-196, <https://doi.org/10.1006/qres.1997.1961>, 1998.
- 1028 Polley, H. W., Johnson, H. B., and Mayeux, H. S.: Nitrogen and water requirements of C3
1029 plants grown at glacial to present carbon dioxide concentrations, *Funct. Ecol.*, 9, 86-96,
1030 <https://doi.org/10.2307/2390094>, 1995.
- 1031 Post-Beittenmiller, D.: Biochemistry and molecular biology of wax production in plants, *Annu.*
1032 *Rev. Plant Biol.*, 47, 405-430, <https://doi.org/10.1146/annurev.arplant.47.1.405>, 1996.
- 1033 Prah, F.G. and Wakeham, S.G.: Calibration of unsaturation patterns in long-chain ketone
1034 compositions for palaeotemperature assessment, *Nature*, 330, 367-369,
1035 <https://doi.org/10.1038/330367a0>, 1987.



- 1036 Prentice, I.C. and Cramer, W.: Harrison SP, Leemans R, Monserud RA, Solomon A M. Global
1037 biome model: predicting global vegetation patterns from plant physiology and dominance,
1038 soil properties and climate, *J. Biogeography*, 19, 117-134, <https://doi.org/10.2307/2845499>,
1039 1992.
- 1040 Prentice, I.C. and Harrison, S.P.: Ecosystem effects of CO₂ concentration: evidence from past
1041 climates, *Clim. Past*, 5, 297-307, <https://doi.org/10.5194/cp-5-297-2009>, 2009, 2009.
- 1042 Prentice, I.C., Cleator, S.F., Huang, Y.H., Harrison, S.P., and Roulstone, I.: Reconstructing
1043 ice-age palaeoclimates: Quantifying low-CO₂ effects on plants, *Glob. Planet. Change*, 149,
1044 166-176, <https://doi.org/10.1016/J.GLOPLACHA.2016.12.012>, 2017.
- 1045 Prentice, I.C., Farquhar, G.D., Fasham, M.J.R., Goulden, M.L., Heimann, M., Jaramillo, V.J.,
1046 Khashgji, H.S., LeQuéré, C., Scholes, R.J., and Wallace, D.W.: *The carbon cycle and*
1047 *atmospheric carbon dioxide*, University Press, Cambridge, 2001.
- 1048 Prentice, I.C., Harrison, S.P., and Bartlein, P.J.: Global vegetation and terrestrial carbon cycle
1049 changes after the last ice age, *New Phytol.*, 189, 988-998, [https://doi.org/10.1111/j.1469-](https://doi.org/10.1111/j.1469-8137.2010.03620.x)
1050 [8137.2010.03620.x](https://doi.org/10.1111/j.1469-8137.2010.03620.x), 2011.
- 1051 Quezel, P.: *Reflexions sur l'évolution de la flore et de la vegetation au Maghreb mediterraneen*,
1052 *Ibis Press*, Paris, 2002.
- 1053 R Development Core Team R: *A Language and Environment for Statistical Computing*. R
1054 Foundation for Statistical Computing, Vienna, Austria, <https://www.R-project.org/>, 2020.
- 1055 Ramstein, G., Kageyama, M., Guiot, J., Wu, H., Hély, C., Krinner, G., and Brewer, S.: How
1056 cold was Europe at the Last Glacial Maximum? A synthesis of the progress achieved since
1057 the first PMIP model-data comparison, *Clim. Past*, 3, 331-339, [https://doi.org/10.5194/cp-](https://doi.org/10.5194/cp-3-331-2007)
1058 [3-331-2007](https://doi.org/10.5194/cp-3-331-2007), 2007.
- 1059 Randall, J.D., Michael, L.R., Tim, R., McVicar, G., and Farquhar, D.D.: Impact of CO₂
1060 fertilisation on maximum foliage cover across the globe's warm, arid environments,
1061 *Geophys. Res. Lett.*, 40, 3031-3035, <https://doi.org/10.1002/grl.50563>, 2013.
- 1062 Reille, M.: *Pollen et spores d'Europe et d'Afrique du nord: Laboratoire de botanique historique*
1063 *et palynologie*, URA CNRS, Marseille, France, 543p., 1992.
- 1064 Reille, M.: *Pollen et spores d'Europe et d'Afrique du Nord (Vol. 2), Laboratoire de Botanique*
1065 *historique et Palynologie*, URA CNRS, Marseille, France, 1995.
- 1066 Reimer, P.J., Bard, E., Bayliss, A., Beck, J.W., Blackwell, P.G., Ramsey, C.B., Buck, C.E.,
1067 Cheng, H., Edwards, R.L., Friedrich, M., and Grootes, P.M.: IntCal13 and Marine13
1068 radiocarbon age calibration curves 0-50,000 years cal BP, *Radiocarbon*, 55, 1869-1887,
1069 https://doi.org/10.2458/azu_js_rc.55.16947, 2013.
- 1070 Rodrigues, T., Alonso-García, M., Hodell, D.A., Rufino, M., Naughton, F., Grimalt, J.O.,
1071 Voelker, A.H.L., and Abrantes, F.: A 1-Ma record of sea surface temperature and extreme
1072 cooling events in the North Atlantic: A perspective from the Iberian Margin, *Quaternary Sci.*
1073 *Rev.*, 172, 118-130, <https://doi.org/10.1016/j.quascirev.2017.07.004>, 2017.
- 1074 Rodrigues, T., Grimalt, J.O., Abrantes, F., Naughton, F., and Flores, J.A.: The last glacial-
1075 interglacial transition (LGIT) in the western mid-latitudes of the North Atlantic: Abrupt sea
1076 surface temperature change and sea level implications, *Quaternary Sci. Rev.*, 29, 1853-
1077 1862, <https://doi.org/10.1016/j.quascirev.2010.04.004>, 2010.
- 1078 Roucoux, K.H., De Abreu, L., Shackleton, N.J., and Tzedakis, P.C.: The response of NW
1079 Iberian vegetation to North Atlantic climate oscillations during the last 65 kyr, *Quaternary*
1080 *Sci. Rev.*, 24, 1637-1653, <https://doi.org/10.1016/j.quascirev.2004.08.022>, 2005.
- 1081 Sage, R.F. and Cowling, S.A.: Implications of stress in low CO₂ atmospheres of the past: Are
1082 today's plants too conservative for a high CO₂ world?, in: *Carbon dioxide and environmental*



- 1083 stress, edited by: Luo, Y., Mooney, H.A., Academic Press, New York, 289- 305,
1084 <https://doi.org/10.1016/B978-012460370-7/50012-7>, 1999.
- 1085 Salgueiro, E., Naughton, F., Voelker, A.H.L., de Abreu, L., Alberto, A., Rossignol, L., Duprat,
1086 J., Magalhães, V.H., Vaqueiro, S., Turon, J.L., and Abrantes, F.: Past circulation along the
1087 western Iberian margin: a time slice vision from the Last Glacial to the Holocene,
1088 *Quaternary Sci. Rev.*, 106, 316-329, <https://doi.org/10.1016/j.quascirev.2014.09.001>,
1089 2014.
- 1090 Sánchez Goñi, M.F., Cacho, I., Turon, J.L., Guiot, J., Sierro, F.J., Peyrouquet, J.P., Grimalt,
1091 J.O., and Shackleton, N.J.: Synchronicity between marine and terrestrial responses to
1092 millennial scale climatic variability during the last glacial period in the Mediterranean region,
1093 *Clim. Dynam.*, 19, 95-105, <https://doi.org/10.1007/s00382-001-0212-x>, 2002.
- 1094 Shakun, J.D., Clark, P.U., He, F., Marcott, S.A., Mix, A.C., Liu, Z., Otto-Bliesner, B.,
1095 Schmittner, A., Bard, E.: Global warming preceded by increasing carbon dioxide
1096 concentrations during the last deglaciation, *Nature*, 484, 49-54,
1097 <https://doi.org/10.1038/nature10915>, 2012.
- 1098 Shao, Y., Anhäuser, A., Ludwig, P., Schlüter, P., and Williams, E.: Statistical reconstruction of
1099 global vegetation for the last glacial maximum, *Glob. Planet. Change*, 168, 67-77,
1100 <https://doi.org/10.1016/j.gloplacha.2018.06.002>, 2018.
- 1101 Simpson, G.L.: Modelling palaeoecological time series using generalised additive models,
1102 *Front. Eco. Evo.*, 6, 149, <https://doi.org/10.3389/fevo.2018.00149>, 2018.
- 1103 Sitch, S., Smith, B., Prentice, I.C., Arneeth, A., Bondeau, A., Cramer, W., Kaplan, J.O., Levis,
1104 S., Lucht, W., Sykes, M.T., Thonicke, K., and Venevsky, S.: Evaluation of ecosystem
1105 dynamics, plant geography and terrestrial carbon cycling in the LPJ dynamic global
1106 vegetation model, *Glob. Chang. Biol.*, 9, 161-185, <https://doi.org/10.1046/j.1365-2486.2003.00569.x>, 2003.
- 1108 Stockmarr, J.A.: Tablets with spores used in absolute pollen analysis, *Pollen spores*, 13, 615-
1109 621, 1971.
- 1110 Street-Perrott, F.A., Huang, Y., Perrott, A., Eglinton, G., Barker, P., Khelifa, L.B, Harkness,
1111 D.D., Olago, D.O.: Impact of lower atmospheric carbon dioxide on tropical mountain
1112 ecosystems, *Science*, 278, 1422-1426, <https://doi.org/10.1126/science.278.5342.1422>,
1113 1997.
- 1114 Stuiver, M., Reimer, P.J., and Reimer, R.W., CALIB 7.1 [WWW program]: <https://calib.org>, last
1115 access 7 July 2020.
- 1116 Svenning, J.C., Fløjgaard, C., Marske, K.A., Nógues-Bravo, D., and Normand, S.: Applications
1117 of species distribution modelling to paleobiology, *Quaternary Sci. Rev.*, 30, 2930-2947,
1118 <https://doi.org/10.1016/j.quascirev.2011.06.012>, 2011.
- 1119 Svenning, J.C., Normand, S., and Kageyama, M.: Glacial refugia of temperate trees in Europe:
1120 insights from species distribution modelling, *J. Ecol.*, 96, 1117-1127,
1121 <https://doi.org/10.1111/j.1365-2745.2008.01422.x>, 2008.
- 1122 Tarroso, P., Carrión, J., Dorado-Valiño, M., Queiroz, P., Santos, L., Valdeolillos-Rodríguez,
1123 A., Célio Alves, P., Brito, J.C., and Cheddadi, R.: Spatial Climate Dynamics in the Iberian
1124 Peninsula since 15 000 yr BP, *Clim. Past*, 12, 1137-1149, <https://doi.org/10.5194/cp-12-1137-2016>, 2016.
- 1126 Tognetti, R., Cherubini, P., and Innes, J.L.: Comparative stem-growth rates of Mediterranean
1127 trees under background and naturally enhanced ambient CO₂ concentrations, *New Phytol.*,
1128 146, 59-74, <https://doi.org/10.1046/j.1469-8137.2000.00620.x>, 2008.
- 1129 Tripathi, A.K., Roberts, C.D., and Eagle, R. A.: Coupling of CO₂ and Ice Sheet Stability Over
1130 Major Climate Transitions of the Last 20 Million Years, *Science*, 326, 1394-1397.



- 1131 <https://doi.org/10.1126/science.1178296>, 2009.
- 1132 Turon, J.L., Lézine, A.M., and Denèfle, M.: Land-sea correlations for the last glaciation inferred
1133 from a pollen and dinocyst record from the Portuguese margin, *Quaternary Res.*, 59, 88-
1134 96, [https://doi.org/10.1016/S0033-5894\(02\)00018-2](https://doi.org/10.1016/S0033-5894(02)00018-2), 2003.
- 1135 van der Knaap, P., Willem, O.; van Leeuwen, J. F.N. Late-Glacial and early-Holocene
1136 vegetation succession, altitudinal vegetation zonation, and climatic change in the Serra da
1137 Estrela, Portugal, *Rev. Paleobot. Palyno.*, 97, 239-285, [https://doi.org/10.1016/S0034-6667\(97\)00008-0](https://doi.org/10.1016/S0034-6667(97)00008-0), 1997.
- 1139 Villanueva, J. and Grimalt, J.O.: Gas Chromatographic Tuning of the U^{k}_{37} Paleothermometer,
1140 *Anal. Chem.*, 69, 3329-3332, <https://doi.org/10.1021/ac9700383>, 1997.
- 1141 Volkman, J.K., Barrer, S.M., Blackburn, S.I. and Sikes, E.L.: Alkenones in *Gephyrocapsa*
1142 *oceanica*: Implications for studies of paleoclimate, *Geochim. Cosmochim. Ac.*, 59, 513-520,
1143 [https://doi.org/10.1016/0016-7037\(95\)00325-T](https://doi.org/10.1016/0016-7037(95)00325-T), 1995.
- 1144 Ward, J.K.: Evolution and growth of plants in a low CO₂ world, in: A history of atmospheric
1145 CO₂ and its effects on plants, animals, and ecosystems, edited by: Ehleringer, J.R., Cerling,
1146 T.E., Dearing, M.D., Springer, New York, 232-257, 2005.
- 1147 Woillez, M., Kageyama, M., Krinner, G., de Noblet-Ducoudré, N., Viovy, N., and Mancip, M.:
1148 Impact of CO₂ and climate on the Last Glacial Maximum vegetation: results from the
1149 ORCHIDEE/IPSL models, *Clim. Past*, 7, 557-577, <https://doi.org/10.5194/cp-7-557-2011>,
1150 2011.
- 1151 Wood, S. N.: Generalised Additive Models: An Introduction with R, 2nd Edition, Chapman and
1152 Hall/CRC Press, New York, 496p., <https://doi.org/10.1201/9781315370279>, 2017.
- 1153 Woodward, F.I., Lomas, M.R., and Kelly, C.K.: Global climate and the distribution of plant
1154 biomes, *Philos. T. Roy. Soc. B.* 359, 1465-1476, <https://doi.org/10.1098/rstb.2004.1525>,
1155 2004.
- 1156 Wu, H., Guiot, J., Brewer, S., and Guo, Z.: Climatic changes in Eurasia and Africa at the last
1157 glacial maximum and mid-Holocene: reconstruction from pollen data using inverse
1158 vegetation modelling, *Clim. Dyn.*, 29, 211-229, <https://doi.org/10.1007/s00382-007-0231-3>,
1159 2007.
- 1160
- 1161
- 1162
- 1163
- 1164
- 1165
- 1166
- 1167
- 1168
- 1169
- 1170



1171 **Tables and figures**

1172 **Table 1 – Radiocarbon ages of IODP Site U1385.**

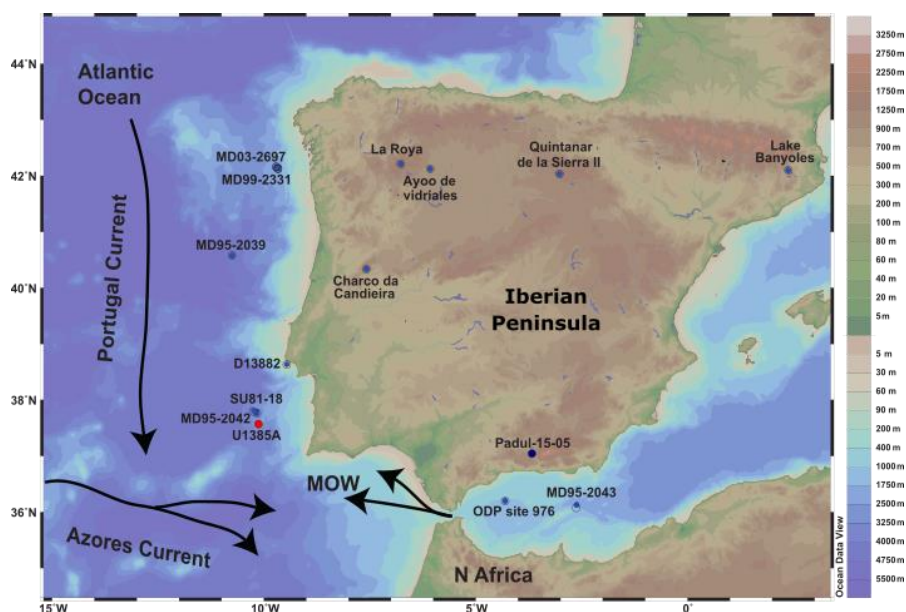
Lab code	Core Depth (cmcd)	Material	Conv. AMS ¹⁴ C (yr B.P.)	Error	Weighted mean deltaR
*20140801r9_MSGforam01_5ox	52	<i>G. bulloides</i>	2525	28	143
*20140801r5_MSGforam01_1ox	108	<i>G. bulloides</i>	6181	35	143
*20140801r6_MSGforam01_2ox	156	<i>G. bulloides</i>	10060	33	143
UCIAMS-219300	186	<i>G. bulloides</i>	11310	60	143
*20140801r7_MSGforam01_3ox	193	<i>G. bulloides</i>	11499	43	143
UCIAMS-219301	217	<i>G. bulloides</i>	12300	40	143
UCIAMS-219302	237	<i>G. bulloides</i>	13430	110	143
*20140801r8_MSGforam01_4ox	246	<i>G. bulloides</i>	13355	45	143
UCIAMS-219303	251	<i>G. bulloides</i>	13670	60	143
UCIAMS-219304	303	<i>G. bulloides</i>	15890	70	143
UCIAMS-219305	333	<i>G. bulloides</i>	17090	90	143

1173 * AMS from Oliveira et al. (2018)

1174



1175



1176

1177 **Figure 1** – Location of the IODP Site U1385 and of the marine and terrestrial pollen records
1178 discussed in the text. Marine sedimentary records: MD03-2697 (Naughton et al., 2016); MD99-
1179 2331 (Naughton et al., 2007); MD95-2039 (Roucoux et al., 2005); D13882 (Gomes et al.,
1180 2020); MD95-2043 (Fletcher and Sánchez Goñi, 2008); MD95-2042 (Chabaud et al., 2014);
1181 SU81-18 (Turon et al., 2003); ODP Site 976 (Comborieut Nebout et al., 1998; 2002; 2009);
1182 Continental sedimentary records: Lake de Banyoles (Pèrez-Obiol and Julià, 1994); Quintanar
1183 de la Sierra II (Peñalba et al., 1997); La Roya (Allen et al., 1996); Ayoo de vidriales (Morales-
1184 Molino and Garcia-Anton, 2014); Charco da Candieira (Van der Knaap and van Leeuwen,
1185 1997); Padul15-05 (Camuera et al., 2019). Black arrows represent the surface water
1186 circulation (MOW, Portugal and Azores Current). Note that coastline boundaries are for the
1187 present day.

1188

1189

1190

1191

1192

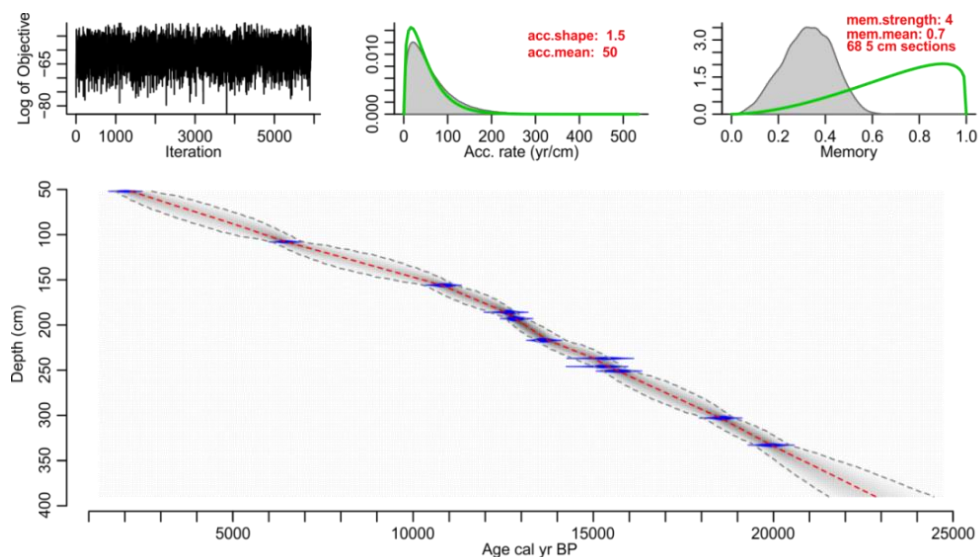
1193

1194



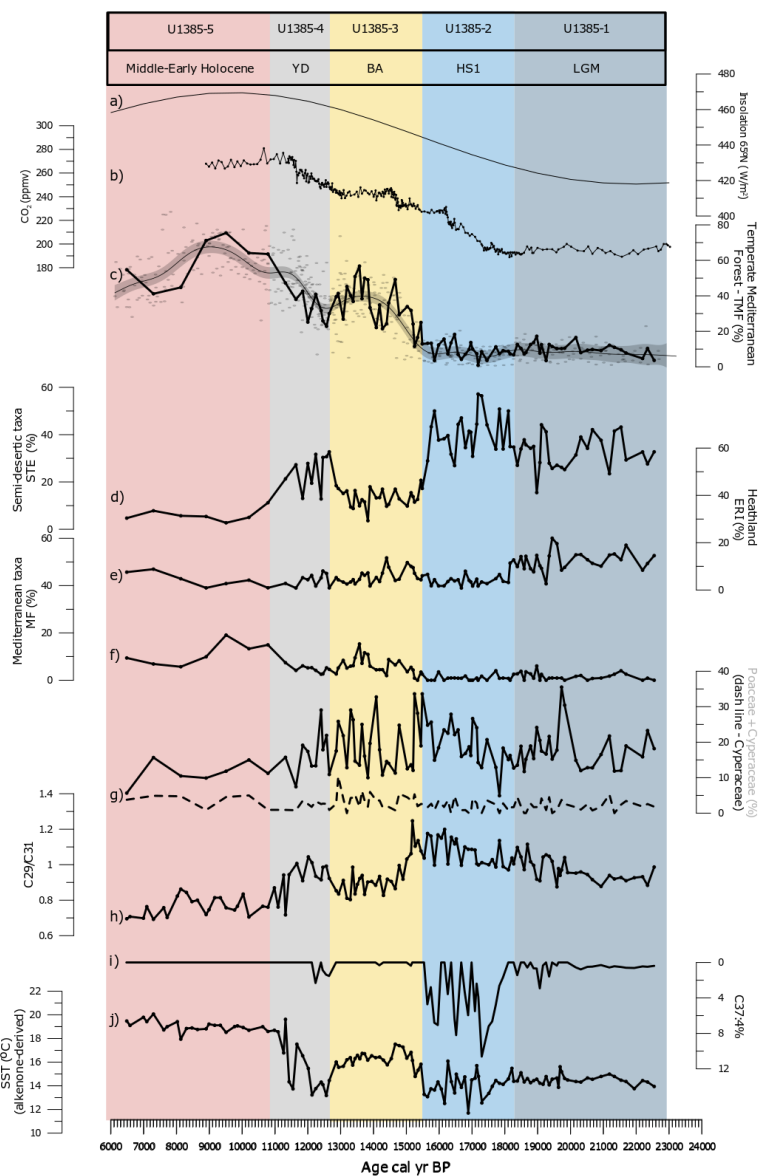
1195

1196



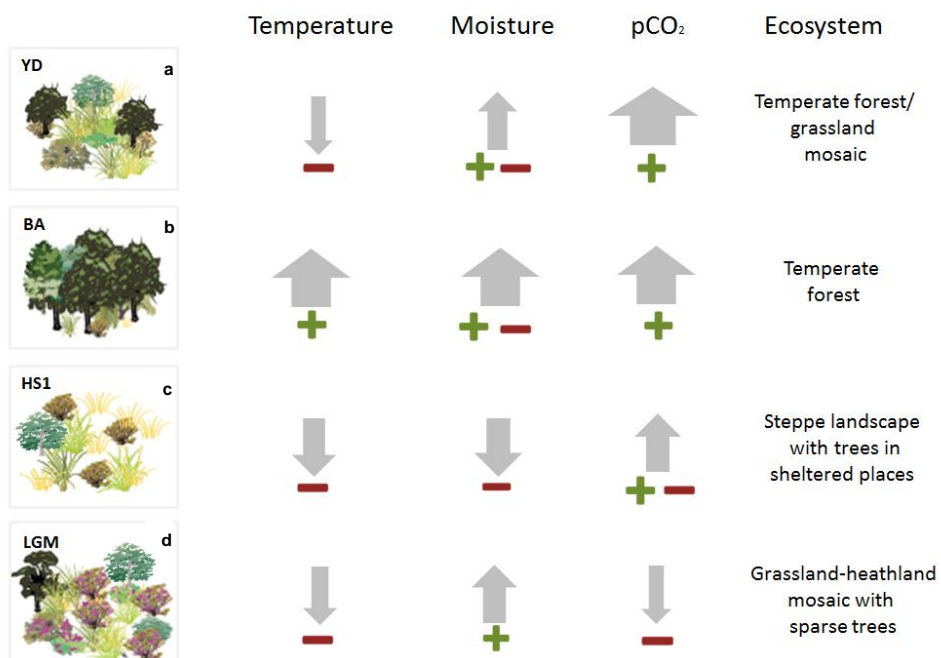
1197

1198 **Figure 2** – Age-depth model for IODP Site U1385 using a Bayesian approach with Bacon
1199 v.2.3.5 (Blaauw and Christen, 2011). The original dates were calibrated using Marine 13.14c
1200 (Reimer et al., 2013) grey stippled line show 95% confidence intervals; red curve shows single
1201 "best" model based on the mean age for each depth. Upper graphs show from left to right:
1202 Markov Chain Monte Carlo (MCMC) iterations and priors (green line) and posteriors (dark grey
1203 line with a grey fill) for the accumulation rate and variability/memory. Note: the depth (Y axis)
1204 was converted to cm from the corrected revised meter composite depth (crmcd).



1205

1206 **Figure 3** – Comparison of multiproxy records from the Site U1385 with 65°N July (W/m^2)
 1207 summer insolation (Berger and Loutre, 1991) and CO₂ composite from WAIS (Marcott et al.,
 1208 2014) ; b) CO₂ (ppmv); Principal pollen-based ecological groups: c) Temperate Mediterranean
 1209 Forest (%) (solid black line) and Compilation of Iberian Margin TMF records (D13882, MD03-
 1210 2697; MD95-2042; MD95-2043; ODP-976; U1385) – GAM (curve with grey (%), d) Semi-
 1211 desertic taxa (%), e) Heathland (%), f) Mediterranean taxa (%) and g) Poaceae + Cyperaceae
 1212 (%; dash line - Cyperaceae); h) C₂₉/C₃₁ ratio, i) C_{37:4} (%) and j) SST (°C). The different coloured shading
 1213 corresponds to the pollen zones (SM Fig.1 and S.M. Table 1) and were connected with the
 1214 periods indicated.



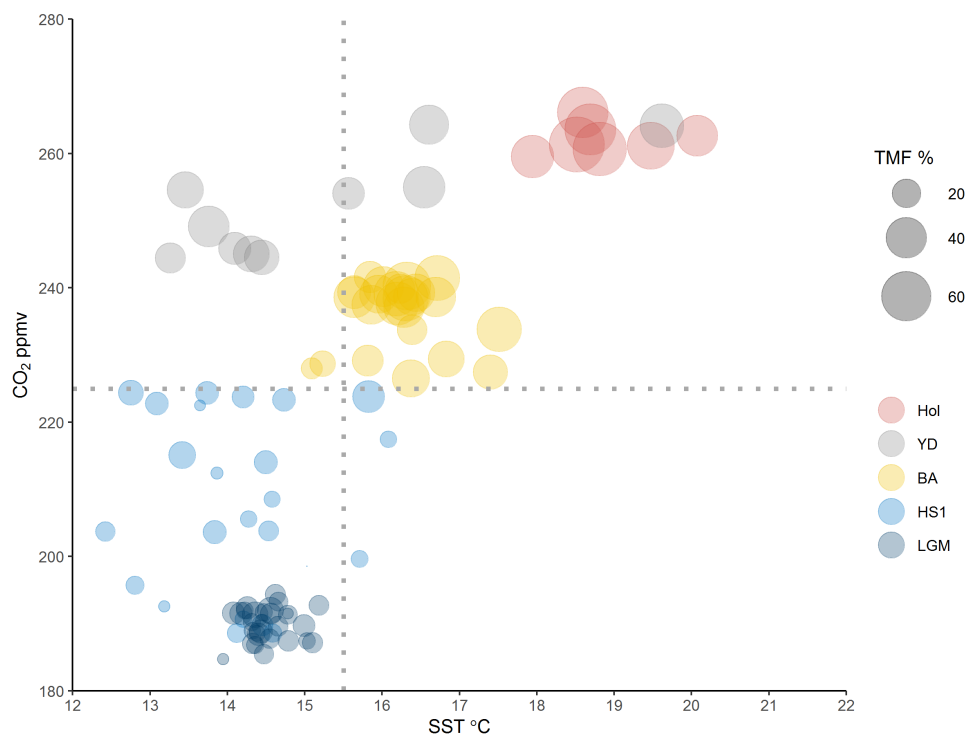
1215

1216

1217 **Figure 4** – Schematic representation of the influence of climatic parameters (precipitation and
1218 temperature) as well as the physiological contribution of CO₂ for each period showing a
1219 schematic reconstruction of the ecosystem scenarios.

1220

1221



1222

1223 **Figure 5** – Dispersion plot showing the relation between CO₂ (Marcott et al., 2014) and SST
1224 in relation to TMF % across the different intervals of the deglaciation, following the pollen
1225 zones boundaries.